17. GEOCHEMISTRY OF SEDIMENTS, LEG 64, GULF OF CALIFORNIA[1]

Jeffrey W. Niemitz, Dickinson College, Carlisle, Pennsylvania

ABSTRACT

Analyses of sediments from Leg 64 sites reveal a diverse and in one case unique geochemistry. Sites are characterized by high heat flow along an active, divergent plate boundary, or rapid accumulation of diatom muds, or both. The geochemical trends of Sites 474–476 at the tip of Baja California reflect changes in the percentages of sedimentary components—particularly biogenous matter and mineralogy—that support interpretations of sedimentary environments inferred to be present since the commencement of subsidence along this young, passive continental margin. The sediments below dolerite sills in Holes 477, 477A, 478, and 481 show major mineralogic and chemical deviations from "average" hemipelagic sediments. The sills appear to have two functions: (1) they allow hydrothermal circulation and metamorphism in a partially closed system by trapping heat and fluids emanating from below, and (2) they expel heated interstitial fluids at the moment of intrusion and mobilize elements, most likely leading to the formation of metalliferous deposits along the surface traces of normal faults in the basin. The hydrothermal system as a whole appears to be localized and ephemeral, as is indicated by the lack of similar geochemical trends and high heat flow at Sites 478 and 481. Site 479 illustrates sedimentation in an oxygen-minimum zone with anoxic sediments and concomitant geochemical trends, especially for MnO. With few exceptions, geochemical trends are remarkably constant with depth, suggesting that Site 479 can serve as an "internal" standard or average sediment against which the magnitude of hydrothermal alteration at the basinal Sites 477, 478, and 481 can be measured.

INTRODUCTION

The unique combination of tectonic, hydrographic, and sedimentologic processes in the Gulf of California produces a geochemical environment heretofore undefined. Eight sites drilled by the *Glomar Challenger*, seven of which will be discussed here, provide an excellent opportunity to study geochemical trends in hemipelagic sediments on a rapidly subsiding, passive, continental margin, in an active tectonic basin, and in an oxygen-minimum zone of a continental slope.

Of particular interest is the interaction of an active, divergent plate boundary with exceptionally high heat flow (Lawver et al., 1975), hemipelagic sediments accumulating at high rates (Fig. 1) and a doleritic sill injected into the sediments in the Guaymas Basin of the central Gulf. Can the hydrothermal circulatory system suggested by the heat flow distribution (Williams et al., 1979) be documented geochemically? If so, what is the nature of this hydrothermal system within the Guaymas Basin and is it common to all basins in the Gulf of California? How does this system compare and contrast with the Galapagos Mounds or the 21° North East Pacific Rise hydrothermal sites to the south? Can elemental input from hydrothermal sources be detected in the geochemical trends of hemipelagic sediments such as are accumulating in the Gulf of California? If so, what standard could be used to make such a determination?

The geochemistry of hemipelagic sediments is complex because of the effects of diagenesis, leaving aside the effects of hydrothermal alteration. Changes in geochemical trends with depth can be significant within a short distance. Small changes may be missed because of sampling biases. Moreover, the sedimentary geochemistry does not delineate the entire system. Only in combination with interstitial water data (Gieskes et al., this volume, Pt. 2), heat flow data and models of heat dis-

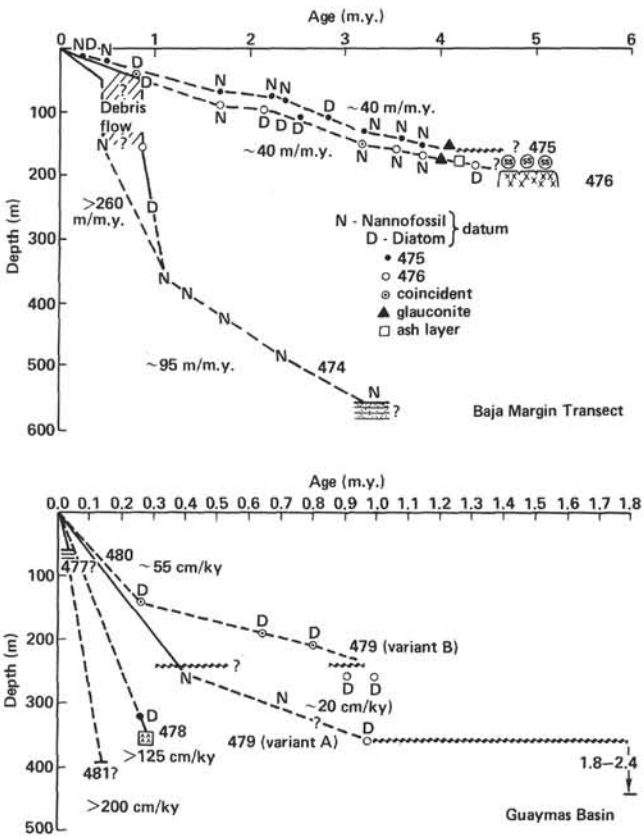

Figure 1. Sedimentation rates at Sites 474–481, determined by biostratigraphic analysis.

[1] Curray, J. R., Moore, D. G., et al., *Init. Repts. DSDP*, 64: Washington (U.S. Govt. Printing Office).

tribution (Williams et al., 1979), physical property data (Einsele, this volume, Pt. 2), and isotopic data (Shanks and Niemitz, this volume, Pt. 2; Kastner, this volume, Pt. 2) can a viable model be developed.

METHODS

From cores at seven sites on Leg 64, 232 10-cm^3 samples were collected. Of these, 79 were analyzed as unwashed, bulk-sediment samples for 18 elements, organic carbon, and loss on ignition (LOI) (Table 1). Samples were ground to less than 200 mesh in an automatic grinder. Carefully weighed aliquots of sample (approx. 0.85 g) were thoroughly homogenized in a Spex mill with boric acid powder (approx. 0.15 g) and pressed into a pellet. All samples and standards were similarly made for analysis by X-ray dispersive spectrometer (Kevex 7000-Micro-X). Samples were counted under vacuum for 100 s. Standards were run at least three times during any particular analysis of an element or elements. Randomly selected samples were run in triplicate to assess precision. Results are presented as oxides for major elements (Table 3) and as elemental concentrations for minor elements.

The USGS standard rocks and sediments analyzed with the samples gave excellent results when compared with the established values of Flanagan (1972, 1976; see Table 2 for comparison). Errors are estimated to be $\pm 6\%$ or less for major elements and $\pm 11\%$ for minor elements. Matrix effects common in analyses of marine sediments seem to be the reason that totals of the major elements are $>100\%$. Selected samples analyzed for Fe, Mn, Cu, Cr, Co, and Zn by atomic absorption spectrophotometry corroborated the X-ray dispersive data.

Organic carbon was determined by analyzing an acid-leached (10% HCl) split of each sample for total carbon, using a digital LECO total carbon analyzer. LOI was measured on oven-dried (110°C) and desiccated samples at 1000°C for 1 hr. Precision was $\pm 1\%$ for both analyses.

Though analytical errors are relatively low, it is still advantageous to present the major elements as oxide ratios (Table 3) with respect to Al_2O_3, which is assumed to be a conservative element derived from one source only—weathering of continental rocks. S and Cl, which constituted a significant part of the bulk, unwashed sediment, were also determined. A correction has been made in the Na_2O content for NaCl in sea water.

GEOCHEMICAL ANALYSES, BY SITE

The seven DSDP sites can be divided into two groups according to their tectonic setting: (1) those that are not associated with the inferred active rift boundary and hence are unaffected by hydrothermal processes (Sites 474, 475, 476, and 479) and (2) those in close proximity to the inferred active rift boundary and hence assumed to have been or to continue to be affected by hydrothermal processes (Sites 477, 478, and 481) (for locations, see Site Chapters, this volume, Pt. 1).

Because of their location and the similarities in their geochemical trends, Sites 474, 475, and 476 will be discussed in combination (Figs. 2–5). The "hydrothermal" sites situated in the Guaymas Basin will be discussed together to facilitate comparisons of the differences suggested by their geochemistry (Figs. 6–16). Site 479 (Figs. 17–20), a unique geochemical and sedimentological environment, is discussed separately because of its proximity to the Guaymas Basin sites and possible use as an "internal" geochemical standard against which deviations in chemistry induced by hydrothermal processes may be measured.

Because of the chemical complexity of hemipelagic sediments, an attempt is made to compare the geochemical trends of these sites with so-called "average" rocks and sediments in order to expose significant deviations. Table 4 shows the derived major oxide ratios and minor element concentrations for an average shale, continental crust (Krauskopf, 1979), and average Terrigenous Matter (TM; Boström et al., 1976). Average values for major oxide ratios and elemental concentrations for each site are included in Table 4 for comparison.

Sites 474, 475, and 476 (Figs. 2–5)

Although the objectives of the three-hole transect at the mouth of the Gulf of California were (1) to study the subsidence history of a passive continental margin and (2) to define the nature of the continental/oceanic crust boundary, the sites also provide an opportunity to examine hemipelagic sedimentation and sedimentary processes on a young continental margin (site chapters, this volume, Pt. 1; Einsele and Kelts, this volume, Pt. 2). The geochemical trends in the sediments here reflect (1) the changes in percentage of sedimentary components, (2) diagenetic and Eh–*p*H conditions, and (3) mineralogy supporting inferences about a variety of sedimentary environments and sedimentation rates before and after the commencement of active rifting in the Gulf 4 Ma.

Commonly, the geochemical trends are similar from site to site (see for example SiO_2, Fe_2O_3, TiO_2, V, and Cu), indicating a common source for the sediment. Many elemental trends suggest a correlation with the percentage of sedimentary components deposited or with the presence or absence of a particular component. CaO (Fig. 4) is a good example. CaO/Al_2O_3 varies widely in the surface sediments, decreasing from Sites 476 to 475 to 474. The amount of calcareous nannofossil matter corresponds well with the geochemical trend. Between 90 and 200 meters sub-bottom depth, CaO/Al_2O_3 ratios for the three sites hover near 0.2, in good agreement with average shale and TM. A major source of Ca from the continent is indicated. However, below 200 meters in Hole 474A (the only data available), the CaO ratio again deviates, with increases occurring at 193 meters and 527 meters. Volcanic ash in the sediments at these depths appears to explain the high CaO/Al_2O_3 values. An alternative explanation may be that the intercalated dolerite sills (basement?) are a source of Ca. Experimental work (Seyfried and Bischoff, 1981) has established that Ca can be exchanged from basalts to sea water under conditions occurring at midocean ridges. If these sediments were deposited before sill injection, it is possible that they are the repository for this excess Ca. High Fe_2O_3/Al_2O_3 ratios in the basal sediments along many segments of midocean ridges should accompany the high CaO/Al_2O_3 ratios. The opposite is in fact observed, suggesting that the high CaO is due to volcanic activity associated with regional tectonism in the late Miocene.

The minor elements Cr and V (Fig. 5) show similar and varied trends. Some significant exceptions appear related to organic carbon, however. The negative correlation of Cr and V concentrations with the percentage of biogenous components in the sediments at Sites 476 (100–165 m) and 474 (100–200 m) suggests that these trends are caused by the dilution of terrigenous sediments with biogenous material of low Cr and V content. Decreases in TiO_2 and MgO provide supporting evidence. Organic carbon and Cr (also Ni and Co) are posi-

Table 1. Chemical composition of bulk solids, Leg 64.

Sample (interval in cm)	Depth (m)	Major Oxides (wt.%)													Minor Elements							
		SiO_2	Al_2O_3	Fe_2O_3	MgO	K_2O	CaO	Na_2O	TiO_2	P_2O_5	MnO	Loss on Ignition	S	Total	Cl (%)	C_{org} (%)	Co (ppm)	Cr (ppm)	Cu (ppm)	Ni (ppm)	V (ppm)	Zn (ppm)
Hole 474																						
1-1, 54-56	0.55	51.45	12.41	5.87	2.51	3.12	3.67	1.03	0.67	0.21	0.11	16.15	1.06	98.26	2.59	1.69	10	85	88	106	218	250
11-2, 109-111	90.10	57.45	12.90	6.69	2.44	3.09	2.12	1.69	0.79	0.32	0.08	14.22	1.33	103.13	1.41	0.79	18	104	118	93	321	267
17-5, 110-112	151.61	58.32	14.17	5.89	2.25	3.25	4.40	1.71	0.71	0.23	0.12	13.28	1.16	105.49	1.29	1.58	12	76	75	78	218	242
Hole 474A																						
4-1, 99-101	193.00	47.23	11.73	5.22	2.04	2.71	10.73	1.30	0.59	0.30	0.17	17.76	1.31	101.09	1.24	3.54	8	63	60	81	103	166
10-1, 88-90	249.89	50.49	12.28	7.23	2.18	2.77	5.47	1.60	0.75	0.27	0.10	14.94	1.39	99.47	1.11	0.01	15	77	75	82	164	211
16-5, 133-135	313.34	47.42	13.48	6.45	2.25	2.86	7.61	1.55	0.74	0.60	0.13	13.75	1.45	98.29	0.98	1.96	19	75	45	55	172	155
29-1, 74-76	420.75	52.38	13.66	8.79	2.74	3.17	2.31	1.64	0.78	0.27	0.78	13.25	1.13	100.90	0.88	1.66	26	104	142	153	206	408
39-3, 30-32	518.31	55.56	13.59	6.09	3.20	3.42	3.66	1.94	0.65	0.33	0.18	8.88	0.89	98.39	0.89	0.99	19	93	119	141	128	299
39-3, 129-131	519.30	56.26	13.54	7.87	3.81	3.84	1.38	1.99	0.75	0.32	0.49	7.26	0.69	98.20	0.92	0.85	18	86	98	125	208	149
40-2, 127-129	527.28	50.14	12.61	3.89	2.29	3.21	9.39	1.98	0.49	0.32	0.85	12.53	1.26	98.96	1.21	1.55	9	47	53	72	33	158
41-5, 127-129	541.28	52.37	13.29	6.17	3.49	4.17	3.51	1.71	0.67	0.22	0.21	7.55	0.82	94.18	1.00	0.71	19	93	102	116	199	207
Hole 475																						
2-4, 112-114	11.63	52.46	12.38	4.37	2.04	2.92	6.59	0.93	0.55	0.33	0.07	14.24	1.22	98.10	2.27	2.56	11	68	56	66	133	172
11-6, 69-71	99.70	55.61	13.36	5.95	2.88	3.03	2.83	2.01	0.68	0.28	0.09	12.57	1.04	100.33	1.33	0.88	18	94	86	108	204	268
Hole 476																						
1-6, 90-92	8.41	45.22	11.72	4.96	1.96	2.94	12.40	0.65	0.59	0.24	0.07	18.88	0.80	100.43	2.33	1.45	12	60	63	70	128	219
10-4, 99-101	90.50	53.32	14.26	6.53	2.30	2.96	2.13	0.94	0.70	0.25	0.08	12.94	1.52	97.93	1.59	1.60	11	109	83	144	274	321
13-4, 148-150	119.49	54.15	13.58	5.76	2.88	3.11	6.09	1.53	0.71	0.30	0.14	13.03	1.06	102.34	1.33	0.86	20	105	76	112	241	240
18-3, 94-96	164.95	65.34	9.46	3.58	1.08	2.79	2.15	1.90	0.29	0.18	0.09	10.68	0.83	98.37	1.87	1.44	7	30	44	46	10	200
21-4, 23-25	194.24	58.10	13.84	6.72	2.25	4.58	1.37	2.01	0.67	0.56	0.04	9.67	1.94	101.75	1.09	0.43	9	186	65	95	261	212
21-4, 47-49	194.48	49.33	11.90	6.97	1.80	4.06	2.73	1.64	0.52	2.15	0.04	16.73	2.55	100.42	1.34	2.91	23	237	64	182	95	222
Hole 477																						
2-3, 70-72	4.71	52.74	13.90	5.84	3.19	2.75	3.47	1.94	0.76	0.40	0.09	14.01	1.11	100.20	2.31	2.13	15	45	39	46	106	140
7-1, 29-31	48.80	53.11	10.64	3.77	3.00	2.06	6.78	1.09	0.50	0.34	0.14	15.92	1.75	99.10	2.08	1.76	6	63	45	65	27	162
7,CC	50.90	51.54	13.56	7.00	8.32	0.48	5.44	2.46	1.19	0.32	0.09	4.82	0.64	95.86	1.39	0.70	19	112	43	84	189	60
15-1, 3-5	105.54	52.26	13.49	5.46	8.97	3.15	2.48	1.62	0.77	0.33	0.13	10.88	1.88	101.42	1.12	1.08	13	51	39	35	150	130
15-1, 51-53	106.02	53.28	14.06	6.05	5.11	3.34	2.76	1.61	0.81	0.39	0.14	11.09	1.71	100.35	1.06	1.07	12	44	44	47	101	116
15-1, 98-100	106.49	58.23	14.88	5.92	4.19	3.15	0.73	1.23	0.78	0.31	0.03	9.33	1.57	100.35	1.14	1.07	14	56	49	46	149	171
16-1, 115-117	116.16	51.90	13.90	5.17	5.81	2.68	4.06	0.93	0.64	0.45	0.05	10.18	4.36	100.13	1.08	0.81	14	40	37	25	103	114
16-4, 20-22	119.21	46.12	11.93	8.53	4.44	2.25	12.04	1.54	0.46	1.92	0.04	9.14	7.56	105.97	0.92	0.74	3	20	28	27	10	159
17-1, 13-15	124.64	57.26	15.56	6.12	5.07	3.43	1.19	1.22	0.80	0.32	0.07	7.51	1.85	100.40	1.13	0.73	12	46	40	39	141	133
17-3, 68-70	128.19	56.01	14.52	5.97	5.29	3.94	1.64	2.00	0.82	0.33	0.08	8.00	1.71	100.31	0.95	0.75	14	59	43	44	131	124
19-1, 110-112	144.61	56.90	13.08	4.69	2.95	2.81	6.50	0.95	0.65	0.25	0.08	5.59	0.90	95.35	1.41	0.28	5	58	31	25	133	195
20-1, 98-100	153.99	61.21	15.82	5.57	3.54	3.63	3.07	1.83	0.60	0.30	0.07	6.98	1.04	103.66	0.88	0.95	18	55	38	42	125	137
21-1, 29-31	162.80	58.68	14.65	5.83	5.42	1.94	2.61	3.42	0.66	0.37	0.18	6.12	1.55	101.43	0.91	0.72	13	64	43	53	154	111
22-2, 27-29	173.78	59.27	14.23	6.72	4.14	2.60	3.04	3.13	0.63	0.48	0.12	6.78	2.45	103.59	0.79	0.81	20	70	39	34	188	134
23-1, 49-51	182.00	58.63	12.20	5.94	4.10	2.05	4.67	2.21	0.47	0.36	0.11	8.60	2.18	101.52	0.82	1.50	14	57	45	39	86	148
Hole 477A																						
5-1, 98-100	191.99	62.60	11.86	5.68	5.47	0.14	4.53	2.31	0.55	0.25	0.19	3.45	0.46	97.49	1.32	0.58	14	31	30	27	10	998
9-1, 77-79	229.78	63.60	12.47	7.17	3.33	0.10	4.32	2.39	0.48	0.30	0.17	4.24	1.16	99.73	1.17	0.37	19	51	81	55	10	2122
10-1, 36-38	238.87	61.84	11.42	8.63	3.97	0.08	3.41	2.47	0.47	0.34	0.15	4.61	1.13	98.52	1.05	0.43	22	54	187	74	10	2019
Hole 478																						
2-2, 53-55	5.54	60.67	7.75	2.78	2.05	1.55	5.86	0.20	0.30	0.30	0.49	13.23	1.54	96.72	3.51	3.07	5	47	52	55	12	215
4-5, 60-62	29.11	59.13	12.57	5.36	2.52	2.83	3.00	1.63	0.73	0.36	0.13	12.23	1.62	102.11	1.58	1.27	13	48	46	26	81	139
6-5, 138-140	48.89	62.31	12.15	4.80	2.59	2.53	2.87	1.57	0.69	0.38	0.08	11.89	1.64	103.50	1.53	2.22	11	46	49	37	119	144
8-4, 25-27	65.26	63.22	9.51	3.54	1.83	1.92	3.86	0.78	0.41	0.28	0.05	14.99	1.30	101.69	1.75	1.48	6	53	47	59	15	140
12-1, 57-59	99.08	61.80	8.51	3.28	1.58	1.63	2.96	0.66	0.36	0.32	0.36	16.18	1.34	98.98	2.46	2.49	1	46	51	41	10	170
15-4, 90-92	132.41	57.87	11.27	5.34	2.26	2.44	2.83	1.26	0.71	0.35	0.10	12.49	1.71	98.63	1.36	1.34	20	51	42	33	136	145
22-3, 104-106	188.05	58.43	9.98	3.20	1.92	2.06	7.76	1.22	0.44	0.38	0.29	13.96	1.21	100.85	1.79	1.95	1	36	46	59	13	162
29-1, 41-43	250.92	59.87	10.46	3.91	1.97	1.88	5.07	0.50	0.49	0.36	0.12	14.49	1.68	100.80	1.55	2.12	9	64	52	64	40	171
29-2, 123-125	253.24	67.35	11.09	4.47	3.02	1.93	2.27	2.56	0.59	0.35	0.06	6.25	0.73	100.67	0.91	1.37	16	75	56	39	81	100
29-2, 140-142	253.45	62.28	10.28	4.06	2.61	2.15	6.03	1.05	0.55	0.47	0.13	9.36	1.36	100.33	1.12	1.47	10	63	54	84	46	160
30-1, 39-41	256.90	61.07	11.41	3.77	2.09	2.13	3.80	2.03	0.59	0.41	0.15	11.15	1.32	99.92	1.28	1.20	6	65	48	59	72	149
30-2, 118-120	259.19	60.44	9.23	4.39	1.90	1.75	4.74	0.95	0.46	0.34	0.41	15.64	1.35	101.60	1.45	2.21	8	55	44	60	22	146
40-1, 78-80	336.79	67.59	8.98	2.67	1.86	1.67	4.76	1.55	0.38	0.32	0.28	8.91	1.13	100.10	0.72	1.08	6	41	53	63	10	184
40-2, 107-109	338.58	66.27	12.29	3.11	3.43	3.20	1.23	1.67	0.79	0.38	0.09	5.93	1.18	99.57	0.68	1.08	4	68	43	44	163	155
40-2, 133-135	338.84	68.16	13.43	2.93	4.15	3.27	1.50	2.00	0.83	0.36	0.07	4.03	0.78	101.51	0.62	0.26	4	64	55	55	165	151
40-3, 115-117	340.17	16.64	4.89	1.83	25.68	0.10	30.41	0.72	0.12	0.14	0.52	18.49	1.14	100.68	0.94	2.08	1	6	24	14	10	48
Hole 479																						
3-3, 40-42	15.91	64.64	10.22	2.30	1.04	2.33	2.62	0.87	0.51	0.40	0.03	13.48	1.85	100.29	3.15	2.80	9	58	47	50	24	129
7-5, 91-93	57.42	66.70	9.01	2.99	1.21	1.93	0.87	0.13	0.43	0.37	0.03	14.94	1.66	100.27	3.18	2.65	5	58	52	56	30	136
11-2, 72-74	90.73	65.93	8.09	2.15	1.13	1.35	0.68	0.07	0.29	0.30	0.02	14.66	1.16	95.83	3.25	2.44	5	47	47	72	10	113
14-6, 4-6	124.55	64.74	9.09	2.73	1.81	1.82	2.24	0.62	0.36	0.33	0.02	15.46	1.30	100.52	2.37	2.61	5	55	42	52	15	118
15-4, 12-14	131.13	64.27	9.92	3.56	1.74	2.01	2.06	0.64	0.45	0.32	0.04	15.35	1.46	101.82	2.30	2.88	10	64	46	65	42	143
17-4, 59-61	150.60	70.37	6.67	3.25	1.67	2.78	0.91	1.48	0.47	0.40	0.02	13.71	1.26	102.99	2.64	1.58	6	74	48	62	42	156
19-1, 8-10	164.59	66.53	11.27	3.90	1.73	2.16	2.49	1.33	0.49	0.38	0.03	13.03	1.53	104.87	1.78	1.41	11	63	48	60	69	147
20-6, 8-10	181.59	60.07	11.69	4.46	1.74	2.64	1.81	1.26	0.58	0.37	0.03	14.06	1.66	100.37	1.38	1.19	12	81	48	74	104	164
23-6, 41-43	210.42	60.66	11.96	4.25	1.48	2.51	4.70	0.84	0.51	0.32	0.02	14.46	1.69	103.40	1.35	2.27	10	60	49	58	55	147
28-6, 88-90	258.39	60.47	10.71	3.60	1.53	2.20	2.07	0.96	0.46	0.34	0.03	13.29	1.42	97.08	1.87	2.51	4	71	48	51	62	135
32-2, 53-55	290.04	53.88	8.99	3.88	1.09	1.70	0.77	2.49	0.40	0.44	0.03	21.91	1.77	97.35	2.43	2.57	6	66	44	77	46	155
35-4, 5-7	321.06	62.81	12.88	3.71	1.91	2.50	0.92	1.12	0.58	0.34	0.03	11.73	0.92	99.45	1.20	2.90	9	87	47	55	76	152
39-2, 130-132	357.31	41.63	9.76	17.99	0.63	0.96	2.14	1.20	0.53	0.87	0.02	20.07	8.15	103.95	0.91	0.20	47	23	27	120	31	128
44-4, 112-114	407.63	60.01	12.45	3.79	2.43	2.48	5.94	1.40	0.49	0.35	0.02	11.68	1.06	102.10	1.00	1.85	8	75	47	74	65	153
Hole 481																						
1-1, 102-104	1.03	54.89	12.19	5.30	2.79	2.52	2.97	0.61	0.69	0.32	0.07	15.22	1.23	98.80	2.98	2.06	12	54	43	44	126	141
2-1, 80-82	5.56	73.74	5.83	0.10	0.96	0.80	1.52	0.35	0.06	0.26	0.06	17.31	0.79	101.78	2.87	0.08	1	5	32	19	10	52
4-1, 60-62	14.86	55.85	7.87	2.30	2.12	1.39	6.91	0.44	0.28	0.33	0.03	21.82	1.22	100.56	2.88	4.31	1	38	43	57	10	128
7-2, 6-8	30.07	52.92	7.05	2.60	1.92	1.24	5.04	0.24	0.26	0.34	1.52	23.02	1.54	97.69	4.03	2.23	5	40	57	76	10	240
10-1, 6-8	42.82	54.55	8.02	2.99	2.29	1.49	4.85	0.46	0.33	0.42	0.10	22.51	1.44	99.45	4.61	1.78	2	44	49	65	10	139
Hole 481A																						
1-2, 65-67	44.16	58.24	12.49	6.05	2.90	2.46	3.61	1.50	0.65	0.39	0.19	12.49	1.25	102.22	1.79	1.65	12	51	45	41	91	161
4-2, 45-47	72.46	56.31	12.68	5.54	2.77	2.83	3.99	1.59	0.78	0.35	0.17	11.99	1.00	100.00	1.33	2.05	8	52	46	51	151	162
6-5, 10-12	95.61	56.04	12.12	5.56	2.23	2.39	3.15	1.26	0.72	0.32	0.08	11.99	1.04	96.90	1.29	1.15	14	48	37	38	177	119
10-1, 86-88	128.37	57.88	11.84	5.00	2.53	2.44	3.36	1.72	0.65	0.36	0.05	11.73	1.49	99.05	1.30	1.34	9	58	40	32	130	137
14-3, 22-24	168.72	56.11	13.92	5.88	3.58	2.75	3.15	2.04	0.84	0.37	0.09	10.50	0.91	100.14	1.14	0.80	14	54	38	24	174	131
29-1, 99-101	309.00	58.08	12.74	5.72	2.55	2.81	4.15	1.95	0.79	0.38	0.12	10.65	0.99	100.93	1.08	1.25	15	54	41	40	173	119
33-1, 62-64	346.63	61.32	11.20	4.89	2.95	1.10	4.34	1.76	0.40	0.27	0.23	10.72	0.52	99.70	1.86	0.87	12	55	86	63	41	650

Table 2. Comparison of accepted values for USGS standard samples with values run by author along with Leg 64 samples, with X-ray dispersive-spectrometry analyses (labeled "Leg 64").

Standard	SiO_2 (%)	Al_2O_3 (%)	Fe_2O_3 (%)	MgO (%)	CaO (%)	Na_2O (%)	K_2O (%)	TiO_2 (%)	P_2O_5 (%)	MnO (%)	Co (ppm)	Cr (ppm)	Cu (ppm)	Ni (ppm)	V (ppm)	Zn (ppm)
BCR-1	54.50	13.61	13.40		6.95	3.27	1.68		0.36	0.18	38		18.4	16		120
Leg 64	54.32	13.55	13.44		6.92	3.16	1.73		0.35	0.19	37		25.6	16		120.5
AVG-1			6.80	1.53	4.98	4.26	2.90	1.08	0.49	0.10	14		60	18.5		84
Leg 64			7.14	1.29	5.02	4.38	2.95	1.15	0.51	0.09	18		49	18		83
GR			4.05	2.40			4.50	0.65	0.28	0.06	10			55		
Leg 64			3.94	2.50			4.59	0.72	0.30	0.06	6			55		
G-1	72.64	14.04	1.88	0.38	1.39	3.32	5.48	0.26	0.09	0.03	2.5					
Leg 64	72.34	14.63	1.62	0.43	1.40	3.17	5.34	0.27	0.09	0.03	2					
GSP-1	67.36	15.25		0.96		2.80		0.70	0.28							
Leg 64	67.82	15.05		1.07		2.71		0.69	0.29							
W1	52.64	15.00	11.09		10.96	2.15	0.64	1.07		0.17		114			264	86
Leg 64	52.66	14.95	10.86		10.79	2.30	0.58	0.99		0.18		116			245	92
MAG-1				2.98	1.50			0.70		0.11	17.6	103	34.4		114	
Leg 64				2.92	1.43			0.73		0.11	18.9	100	37.2		129	
SCO-1			5.27	2.69	2.68	0.91	2.74	0.75			11.3			30	109	
Leg 64			5.55	2.72	2.80	0.90	2.79	0.68			11.3			31	120	
DRN-1												45			225	
Leg 64												46			245	
BR	38.20	10.20			13.80		1.40		1.04	0.20						
Leg 64	38.23	10.11			13.90		1.42		1.03	0.19						
BHVO-1					11.41	2.29	0.55	2.66								102
Leg 64					11.43	2.37	0.49	2.66								97

tively correlated at the base of Site 476, in response to the occurrence of an organic claystone (sapropel?) in Core 476-21. V, however, decreases significantly, suggesting that Cr (and Co and Ni) are more readily adsorbed or chelated in the organic matter of plankton in the surface waters, to be preserved and enriched under reducing conditions in the sediments. A similar situation occurs along the coast of Southwest Africa, where sediments rich in organic matter have accumulated high concentrations of metals (Calvert and Price, 1970). Boström et al. (1974) have shown that whereas Cr and V concentrations are approximately the same in average shales (see Table 4) Cr is enriched approximately 2.5 times in plankton. Similar enrichment is seen at Site 476. The source of the enrichment of V (260 ppm) just above the organic claystone appears to be solely the terrigenous matter shed from the adjacent continent. The Cr and V trends below 200 meters (Site 474) are very similar, showing slight increases that are due to a progressively lower biogenic component with depth. Sharp fluctuations below 500 meters appear to be associated with several sill injections; however, more detailed analyses above and below the sills are needed to corroborate these observations.

The value of MnO (Fig. 4) remains close to that of average sediments and rocks at all sites until approximately 300 meters sub-bottom depth (Site 474). Below 300 meters MnO values fluctuate widely, producing high concentrations of MnO closely correlated with basal sands of mud turbidites (Section 474A-29-1). Eh-*p*H conditions conducive to MnO_2 precipitation (oxic) have occurred. Alternatively, high MnO in Sections 474A-39-3 and 474A-40-2 may be the result of hydrothermal input, as basal metalliferous sediment has formed layers over injected doleritic sills. As previously mentioned, Fe_2O_3 as well as SiO_2, MgO, K_2O, and other heavy metal values do not clearly substantiate this explanation.

At the base of Hole 476, the geochemistry closely follows changes in mineralogy. The occurrence of a glauconitic sand produces a significant increase in K_2O/Al_2O_3 from 100 to 200 meters sub-bottom, with sharper increases in MgO and Fe_2O_3 (Figs. 2–3) at 200 meters depth. P_2O_5 also deviates from average P_2O_5/Al_2O_3 values in response to a phosphorite layer that was presumably deposited when this site was bathymetrically shallow (proto-Gulf stage?) and isolated (tectonically?) from sediment accumulation in the early Pliocene or possibly the late Miocene. Other than previously noted, SiO_2, MgO, TiO_2, and Na_2O ratios show little deviation from average TM.

Sites 477, 478, and 481 (Figs. 6–16)

Sites 477, 478, and 481 are situated in the southern trough, northwest flank, and northern trough of the Guaymas Basin. Holes 477 and 477A exhibit unusually high heat flow (up to 70 HFU; Becker, 1981), rapid sedimentation rates possibly exceeding 1200 m/m.y. (Fig. 1), and one or more dolerite sills that, it is inferred, were injected into the sediment column. Olive green diatom muds and diatomaceous oozes dominate the sediments above the sills. However, adjacent to and in one case (Site 477) continuing below the sill to the termination depth, the sediments are altered to brownish gray, gray, and grayish black, with significant mineralogical changes. The extreme occurs at Site 477 where the mineralogy includes a zone of anhydrite–calcite–dolomite just below the sill, grading to predominantly illite–chlorite–py-

Table 3. Bulk solids: Elemental oxide ratios to Al_2O_3.

Sample (interval in cm)	Depth (m)	SiO_2 / Al_2O_3	Fe_2O_3 / Al_2O_3	MgO / Al_2O_3	K_2O / Al_2O_3	CaO / Al_2O_3	Na_2O / Al_2O_3	TiO_2 / Al_2O_3	P_2O_5 / Al_2O_3
Hole 474									
1-1, 54-56	0.55	4.15	0.47	0.20	0.25	0.30	0.08	0.054	0.017
11-2, 109-111	90.10	4.45	0.52	0.19	0.24	0.17	0.13	0.061	0.025
17-5, 110-112	151.61	4.12	0.42	0.16	0.23	0.31	0.12	0.050	0.016
Hole 474A									
10-1, 88-90	249.89	4.11	0.59	0.18	0.23	0.45	0.13	0.061	0.022
16-5, 133-135	313.34	3.52	0.48	0.17	0.21	0.56	0.12	0.055	0.045
29-1, 74-76	420.75	3.83	0.64	0.20	0.23	0.17	0.12	0.057	0.020
39-3, 30-32	518.31	4.09	0.45	0.24	0.25	0.27	0.14	0.048	0.024
39-3, 129-131	519.30	4.16	0.58	0.28	0.28	0.10	0.15	0.055	0.024
40-2, 127-129	527.28	3.98	0.31	0.18	0.25	0.74	0.16	0.039	0.025
41-5, 127-129	541.28	3.94	0.46	0.26	0.31	0.26	0.13	0.050	0.017
Hole 475									
2-4, 112-114	11.63	4.24	0.35	0.16	0.24	0.53	0.08	0.044	0.027
11-6, 69-71	99.70	4.16	0.45	0.22	0.23	0.21	0.15	0.051	0.021
Hole 476									
1-6, 90-92	8.41	3.86	0.42	0.17	0.25	1.06	0.06	0.050	0.020
10-4, 99-101	90.50	3.74	0.46	0.16	0.21	0.15	0.07	0.049	0.018
13-4, 148-150	119.49	3.99	0.42	0.21	0.23	0.45	0.11	0.052	0.022
18-3, 94-96	164.95	6.91	0.38	0.11	0.30	0.23	0.20	0.031	0.019
21-4, 23-25	194.24	4.20	0.49	0.16	0.33	0.10	0.15	0.048	0.040
21-4, 47-49	194.48	4.15	0.59	0.15	0.34	0.23	0.14	0.044	0.181
Hole 477									
2-3, 70-72	4.71	3.79	0.42	0.23	0.20	0.25	0.14	0.055	0.029
7-1, 29-31	48.80	4.99	0.35	0.28	0.19	0.64	0.10	0.047	0.032
7,CC	50.90	3.80	0.52	0.61	0.04	0.40	0.18	0.088	0.024
15-1, 3-5	105.54	3.87	0.40	0.67	0.23	0.18	0.12	0.057	0.024
15-1, 51-53	106.02	3.79	0.43	0.36	0.24	0.20	0.11	0.058	0.028
15-1, 98-100	106.49	3.91	0.40	0.28	0.21	0.05	0.08	0.052	0.021
16-1, 115-117	116.16	3.73	0.37	0.42	0.19	0.29	0.07	0.046	0.032
16-4, 20-22	119.21	3.87	0.72	0.37	0.19	1.01	0.13	0.039	0.161
17-1, 13-15	124.64	3.68	0.39	0.33	0.22	0.08	0.08	0.051	0.021
17-3, 68-70	128.19	3.86	0.41	0.36	0.27	0.11	0.14	0.056	0.023
19-1, 110-112	144.61	4.35	0.36	0.23	0.21	0.50	0.07	0.050	0.019
20-1, 98-100	153.99	3.87	0.35	0.22	0.23	0.19	0.12	0.038	0.019
21-1, 29-31	162.80	4.01	0.40	0.37	0.13	0.18	0.23	0.045	0.025
22-2, 27-29	173.78	4.17	0.47	0.29	0.18	0.21	0.22	0.044	0.034
23-1, 49-51	182.00	4.81	0.49	0.34	0.17	0.38	0.18	0.039	0.030
Hole 477A									
5-1, 98-100	191.99	5.28	0.48	0.46	0.01	0.38	0.19	0.046	0.021
9-1, 77-79	229.78	5.10	0.59	0.27	0.01	0.35	0.19	0.038	0.024
10-1, 36-38	238.87	5.42	0.76	0.35	0.01	0.30	0.22	0.041	0.030
Hole 478									
2-2, 53-55	5.54	7.83	0.38	0.26	0.20	0.76	0.03	0.039	0.039
4-5, 60-62	29.11	4.70	0.43	0.20	0.23	0.24	0.13	0.058	0.029
6-5, 138-140	48.89	5.13	0.40	0.21	0.21	0.24	0.13	0.057	0.031
8-4, 25-27	65.26	6.65	0.37	0.19	0.20	0.41	0.08	0.043	0.029
12-1, 57-59	99.08	7.26	0.39	0.19	0.19	0.35	0.08	0.042	0.038
15-4, 90-92	132.41	5.13	0.47	0.20	0.22	0.25	0.11	0.063	0.031
22-3, 104-106	188.05	5.85	0.32	0.19	0.21	0.78	0.12	0.044	0.038
29-1, 41-43	250.92	5.72	0.37	0.19	0.18	0.48	0.05	0.047	0.034
29-2, 123-125	253.24	6.07	0.40	0.27	0.17	0.20	0.23	0.053	0.032
29-2, 140-142	253.45	6.06	0.40	0.25	0.21	0.59	0.10	0.054	0.046
30-1, 39-41	256.90	5.35	0.33	0.18	0.19	0.33	0.18	0.052	0.036
30-2, 118-120	259.19	6.55	0.48	0.21	0.19	0.51	0.10	0.050	0.037
40-1, 78-80	336.79	7.53	0.30	0.21	0.19	0.53	0.17	0.042	0.036
40-2, 107-109	338.58	5.39	0.25	0.28	0.26	0.10	0.14	0.064	0.031
40-2, 133-135	338.84	5.08	0.22	0.31	0.24	0.11	0.15	0.062	0.027
40-3, 115-117	340.17	3.40	0.37	5.25	0.02	6.22	0.15	0.025	0.029
Hole 479									
3-3, 40-42	15.91	6.32	0.23	0.10	0.23	0.26	0.09	0.050	0.039
7-5, 91-93	57.42	7.40	0.33	0.13	0.21	0.10	0.01	0.048	0.041
11-2, 72-74	90.73	8.15	0.27	0.14	0.17	0.08	0.01	0.036	0.037
14-6, 4-6	124.55	7.12	0.30	0.20	0.20	0.25	0.07	0.040	0.036
15-4, 12-14	131.13	6.48	0.36	0.18	0.20	0.21	0.06	0.045	0.032
17-4, 59-61	150.60	10.55	0.49	0.25	0.42	0.14	0.22	0.070	0.060
19-1, 8-10	164.59	5.90	0.35	0.15	0.19	0.22	0.12	0.043	0.034
20-6, 8-10	181.59	5.14	0.38	0.15	0.23	0.15	0.11	0.050	0.032
23-6, 41-43	210.42	5.07	0.36	0.12	0.21	0.39	0.07	0.043	0.027
28-6, 88-90	258.39	5.65	0.34	0.14	0.21	0.19	0.09	0.043	0.032
32-2, 53-55	290.04	5.99	0.43	0.12	0.19	0.09	0.28	0.044	0.049
35-4, 5-7	321.06	4.88	0.29	0.15	0.19	0.07	0.09	0.045	0.026
39-2, 130-132	357.31	4.27	1.84	0.06	0.10	0.22	0.12	0.054	0.089
44-4, 112-114	407.63	4.82	0.30	0.20	0.20	0.48	0.11	0.039	0.028
Hole 481									
1-1, 102-104	1.03	4.50	0.43	0.23	0.21	0.24	0.05	0.057	0.026
2-1, 80-82	5.56	12.65	0.02	0.16	0.14	0.26	0.06	0.010	0.045
4-1, 60-62	14.86	7.10	0.29	0.27	0.18	0.88	0.06	0.036	0.042
7-2, 6-8	30.07	7.51	0.37	0.27	0.18	0.71	0.03	0.037	0.048
10-1, 6-8	42.82	6.80	0.37	0.29	0.19	0.60	0.06	0.041	0.052
Hole 481A									
1-2, 65-67	44.16	4.66	0.48	0.23	0.20	0.29	0.12	0.052	0.031
4-2, 45-47	72.46	4.44	0.44	0.22	0.22	0.31	0.13	0.062	0.028
6-5, 10-12	95.61	4.62	0.46	0.18	0.20	0.26	0.10	0.059	0.026
10-1, 86-88	128.37	4.89	0.42	0.21	0.21	0.28	0.15	0.055	0.030
14-3, 22-24	168.72	4.03	0.42	0.26	0.20	0.23	0.15	0.060	0.027
29-1, 99-101	309.00	4.56	0.45	0.20	0.22	0.33	0.15	0.062	0.030
33-1, 62-64	346.63	5.48	0.44	0.26	0.10	0.39	0.18	0.036	0.024

rite, this in turn grading to a quartz–chlorite–epidote–albite–pyrrhotite assemblage from 191 meters to the bottom of the hole (Kelts, this volume, Pt. 2). A comparison with hydrothermal mineralogy observed in drill holes at the Cerro Prieto Geothermal Fields to the north (Hoagland and Elders, 1978) suggests that the presence of epidote indicates no lower than a 300°C temperature of formation below 191 meters. Similar mineralogical trends were not observed at Sites 478 and 481 (see site chapters, this volume, Pt. 1, for further detail); however, the possibility of their existence below the depth drilled cannot be disregarded. A comparison of the geochemical trends of these three sites therefore, allows some discussion about (1) the nature of the inferred hydrothermal system within the Guaymas Basin, (2) the role of the sill intrusions in the system and the effect of those intrusions on high-water-content hemipelagic sediments, and (3) the magnitude of the effect of hot fluids interacting with hemipelagic diatomaceous muds—a mixture heretofore undefined.

The dolerite sills, completely cooled and therefore relatively old, may have been emplaced very near the sediment/water interface. Particularly at Site 477, the sills appear as a boundary between altered sediments and "normal" hemipelagic sediments deposited after sill injection—an assertion corroborated by the sedimentary geochemistry above the sills at the three sites. With minor exceptions, the elements one might expect to be affected by hydrothermal processes are not affected until sediments immediately adjacent to the sills are penetrated. At this point, SiO_2/Al_2O_3 and K_2O/Al_2O_3 decrease, and MgO/Al_2O_3 increases.

Departures from average values for the major oxide ratios are explained by the same factors (% of sediment components and mineralogy) operating at Sites 474–476. Fluctuations of SiO_2/Al_2O_3 (Figure 6) are consistent with a sediment column comprising mud turbidites and abundant diatoms. At and below the sills the trends for SiO_2/Al_2O_3 in the three sites become ambiguous. A slight decrease in SiO_2 occurs at Site 477 just above the sill, whereas the values increase from just below the sill to the bottom of the hole. A similar trend occurs at Site 481; data are lacking just below the sill, but the SiO_2/Al_2O_3 trend increases as basement(?) is approached. Site 478 shows little change in SiO_2 approaching the first sill and little fluctuation in the sediments between the first and second sills. Below the second sill a slight increase is noted until just above basement(?), where a dramatic decrease occurs.

MgO/Al_2O_3 ratios (Fig. 8) for the three sites generally follow a trend opposite to the SiO_2/Al_2O_3 ratios, particularly near sills. At Site 477 large increases are noted above and below the sill. With one exception at Site 478, similar increases are not evident at the other sites. The sample closest to the intrusion (Section 478-40-3) has a MgO/Al_2O_3 ratio of 5.25, an order of magnitude above all other sediments analyzed. An explanation for this anomaly must also satisfy an unusually high CaO/Al_2O_3 ratio (Fig. 10). These results suggest the presence of significant amounts of dolomite, a finding corroborated by smear slide checks.

Table 4. Average major oxide ratios and elemental concentrations for Sites 474–481, compared to average shale, continental crust, and terrigenous matter.

Sediment	SiO_2/Al_2O_3	Fe_2O_3/Al_2O_3	MgO/Al_2O_3	K_2O/Al_2O_3	CaO/Al_2O_3	Na_2O/Al_2O_3	TiO_2/Al_2O_3	P_2O_5/Al_2O_3	MnO (%)	S (wt%)	Cl (wt%)	C_{org} (wt%)	Co (ppm)	Cr (ppm)	Cu (ppm)	Ni (ppm)	V (ppm)	Zn (ppm)
Average shale[a]	2.93	0.39	0.13	0.17	0.20	0.07	0.043	0.010	0.11	0.25	0.017		20	100	50	80	130	90
Average continental crust[a]	3.94	0.50	0.25	0.16	0.37	0.21	0.055	0.016	0.13	0.030	0.013		22	100	50	75	110	70
Terrigenous matter (TM)[b]	3.81	0.42	0.16	0.17	0.24	0.11	0.046	0.012	0.115	0.195	0.016		22.5	100	50	79	125	85
Sites 474–476 (N = 19)	4.19	0.47	0.19	0.26	0.34	0.12	0.048	0.024	0.13 (18)	1.23	1.40	1.45	15	94	80	101	174	230
Site 477 (N = 18)	4.24	0.46	0.35	0.16	0.32	0.14	0.049	0.025	0.11	1.44 (16)	1.20	0.92	14	54	50	45	101	135 (15)
Site 478 (N = 16)	5.85	0.37	0.23 (15)	0.20	0.39 (15)	0.14	0.050	0.034	0.21	1.31	1.52	1.67	8	52	48	49	62	144
Site 479 (N = 14)	6.26	0.45	0.15	0.21	0.20	0.10	0.047	0.040	0.026	1.44 (13)	2.07	2.13	10	63	46	66	48	141
Site 481 (N = 12)	5.93	0.39	0.23	0.19	0.40	0.10	0.047	0.034	0.11 (11)	1.12	2.26	1.63	12	46	46	46	92	139 (11)

Note: Number of samples used to calculate averages (N) given in stub (extraordinary N values in parentheses).
[a] Average of many authors amassed in Krauskopf (1979).
[b] TM = 75% average shale + 25% average continental crust (data from Krauskopf, 1979), after Boström et al. (1976).

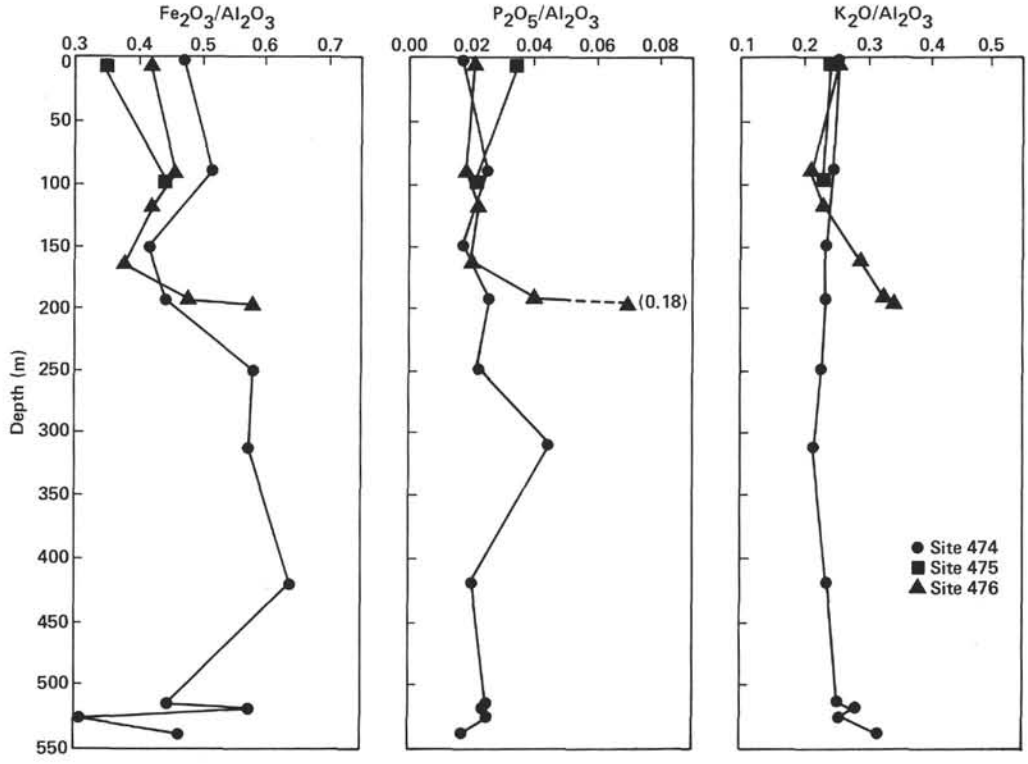

Figure 2. Geochemical trends for Fe_2O_3, P_2O_5, and K_2O at Sites 474, 475, and 476.

K_2O/Al_2O_3 ratios (Fig. 9) at Site 477 appear to exhibit the best evidence for hydrothermal alteration of hemipelagic sediments. Sediments above the upper sill at each site have average oxide ratios of approximately 0.2, quite similar to the ratios for Sites 479 and 474. At Site 477, K_2O decreases just above the sill. No such decrease occurs at Site 481, and Site 478 lacks sufficient data to corroborate a decrease. Below the sills K_2O is essentially quantitatively removed as basement is approached. A smaller decrease was measured at Site 481.

Whereas TiO_2/Al_2O_3 and Na_2O/Al_2O_3 ratios (Table 3) are constant with depth and vary little from average shale and continental crust, CaO/Al_2O_3 (Fig. 10), Fe_2O_3/Al_2O_3 (Fig. 7), and P_2O_5/Al_2O_3 (Fig. 11) show significant excursions. Two alternative explanations that can be cited for the deviations at the three sites are (1) high percentages of sedimentary components (terrigenous or biogenous) not common to these hemipelagic sediments; (2) mineralogy rare in unconsolidated sediments and inferred to be of hydrothermal origin.

The significant fluctuations in ratios of CaO/Al_2O_3, Fe_2O_3/Al_2O_3, and P_2O_5/Al_2O_3 above the sills appear to be explained by changes in the percentage of components of the sediment and texture. For example, Sections 478-2-2 and 478-22-2 exhibit significant deviation from the average for CaO/Al_2O_3 (Table 4). Both are ex-

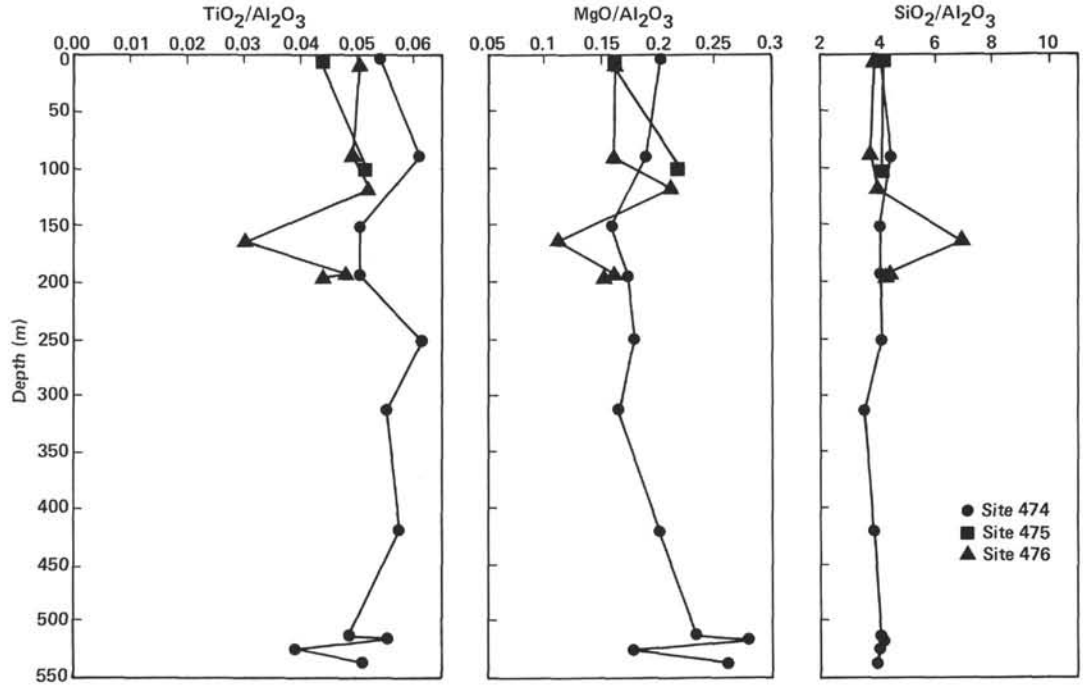

Figure 3. Geochemical trends for TiO_2, MgO, and SiO_2 at Sites 474, 475, and 476.

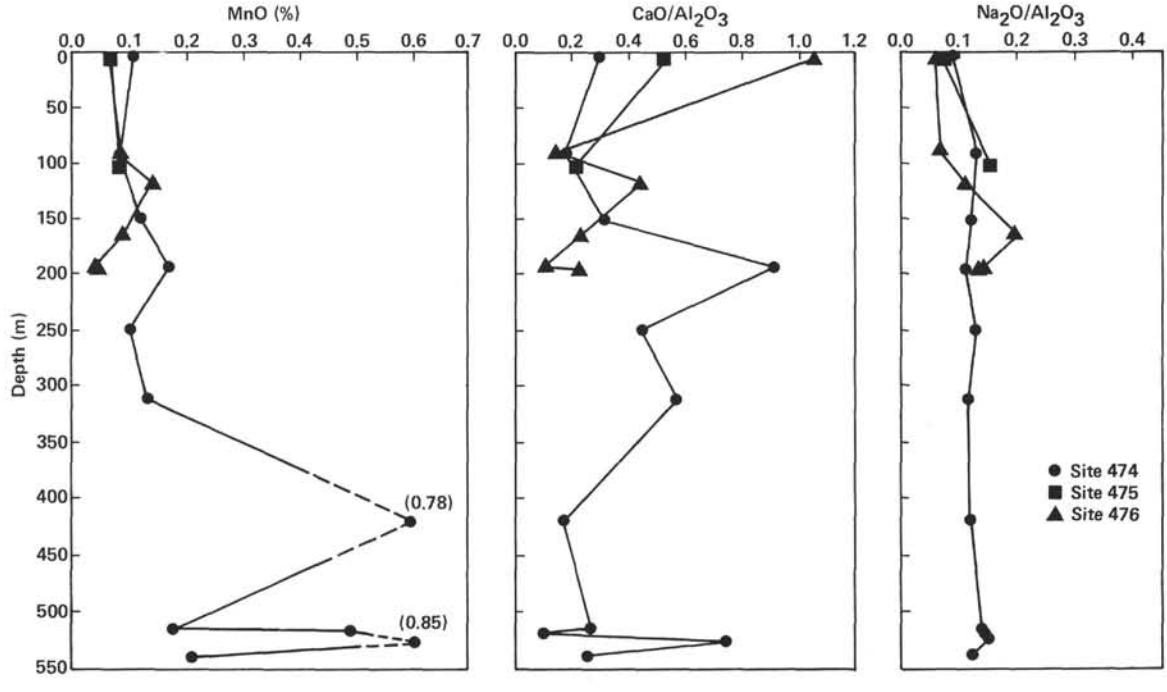

Figure 4. Geochemical trends for MnO, CaO, and Na_2O at Sites 474, 475, and 476.

plained by the occurrence of a high percentage of calcareous nannofossils. Section 481-2-1 shows a very low concentration of Fe_2O_3/Al_2O_3. A coarse basal turbidite sand appears to explain this decrease. P_2O_5 exhibits increased concentrations in the top 50 meters at Site 481 because of increases in organic matter (plant debris) deposited with turbidite sequences.

Large increases in CaO/Al_2O_3 occur again just above basement(?) and above and below the lower sill at Site 478. Similar but smaller increases in Fe_2O_3 and P_2O_5 also occur at this site. As noted earlier, MgO is elevated. Each of these trends appears to be related to the formation of dolomite in the sediment column. The sediment appears "baked," and microscopic, subhedral rhombs of dolomite are clearly visible.

Vanadium (Fig. 13) decreases in concentration as other elements increase. The basis for this behavior is unclear, since comparison with average V values (Table

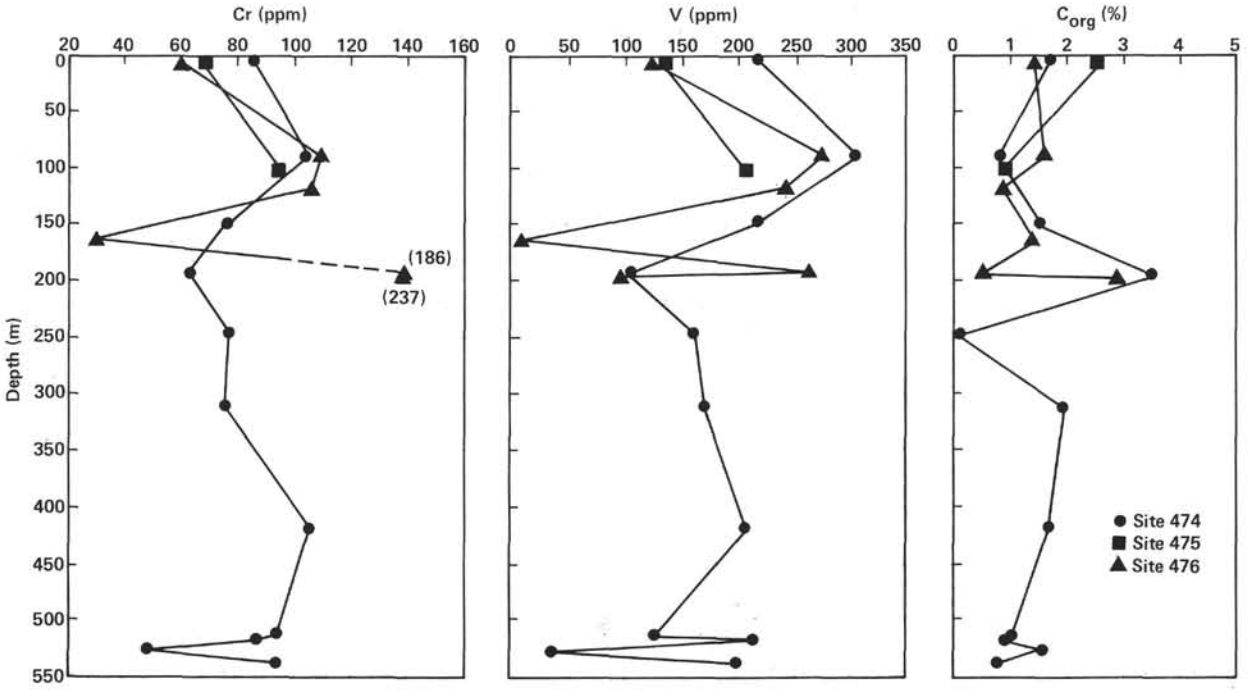

Figure 5. Geochemical trends for Cr, V, and organic carbon at Sites 474, 475, and 476.

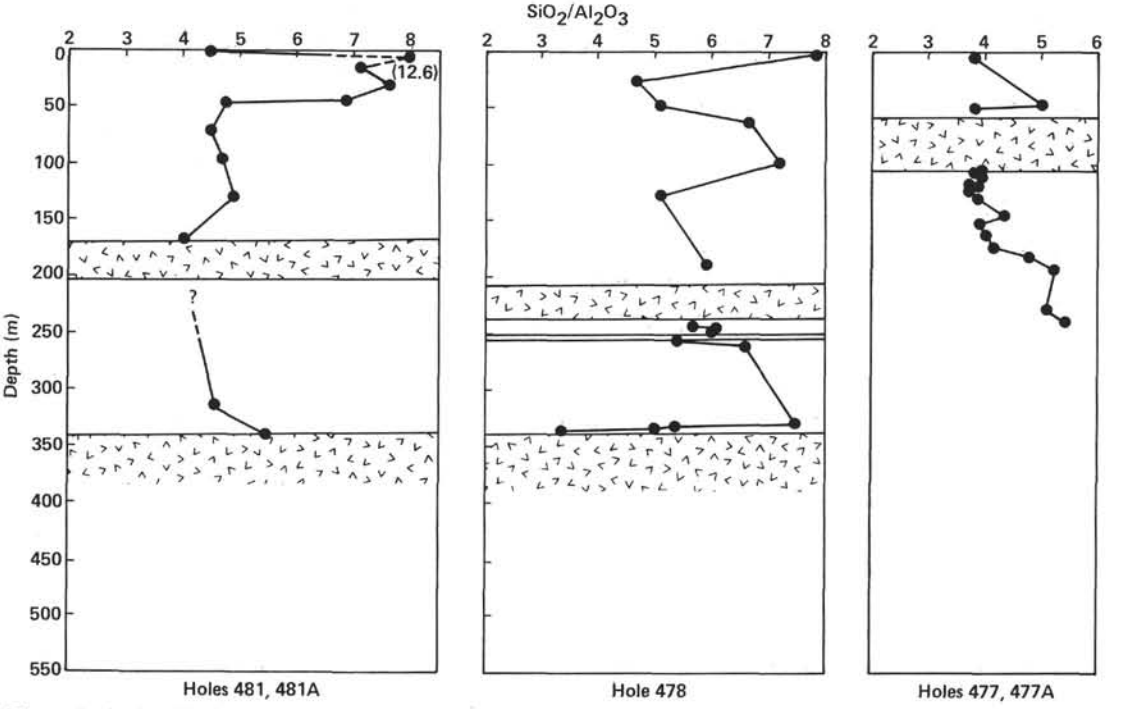

Figure 6. Geochemical trends for SiO_2 at Sites 477, 478, and 481.

4) is not strictly valid because of the biogenous dilution of terrigenous material. However, where nearly quantitative removal of V is coincident with dolerite sills or basement, the data suggest that hydrothermal activity associated with these intrusions is removing V from the continentally derived sediments. Whether V is elevated in interstitial waters is unknown, but it is unlikely. It is more probable that V is mobilized and reprecipitated with hydrothermal pyrite; evidence for this is seen in the consistently high V concentrations at Site 477 between the sill and 191 meters, the pyrite-dominant zone. Unfortunately, similar trends are ambiguous at the other sites. Geochemical trends for V below the sill at Site 481 remain at or near the average for TM.

Section 477-16-4 exhibits unusual deviation from average hemipelagic elemental and oxide ratio values. P_2O_5

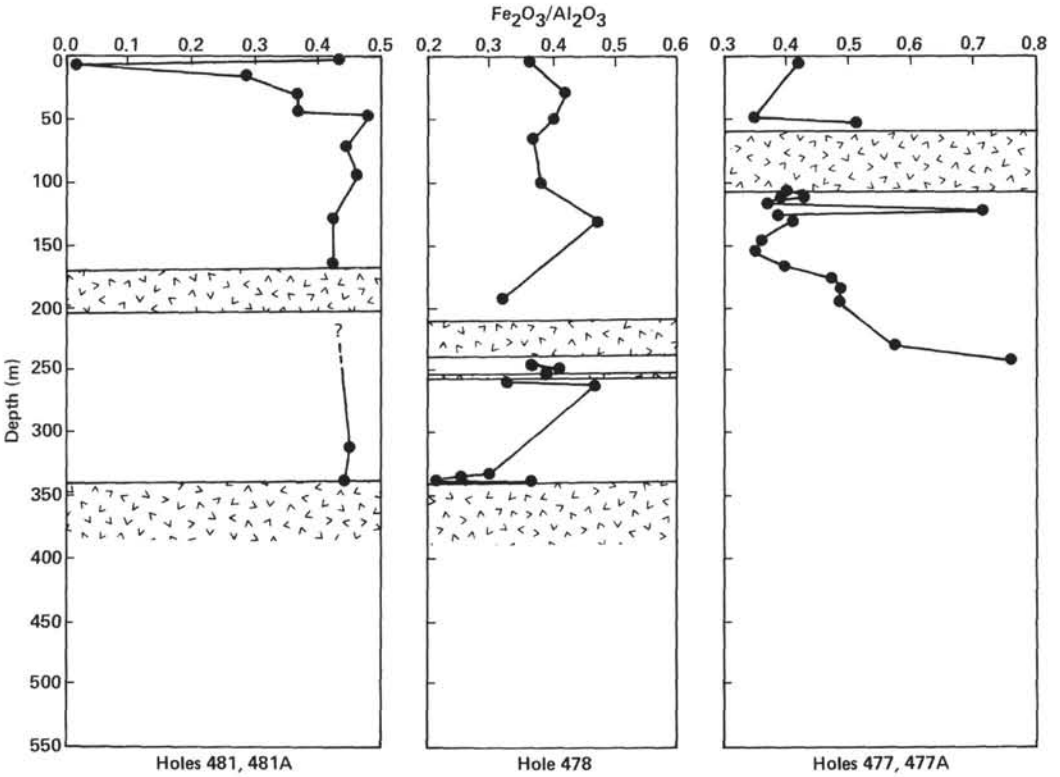

Figure 7. Geochemical trends for Fe_2O_3 at Sites 477, 478, and 481.

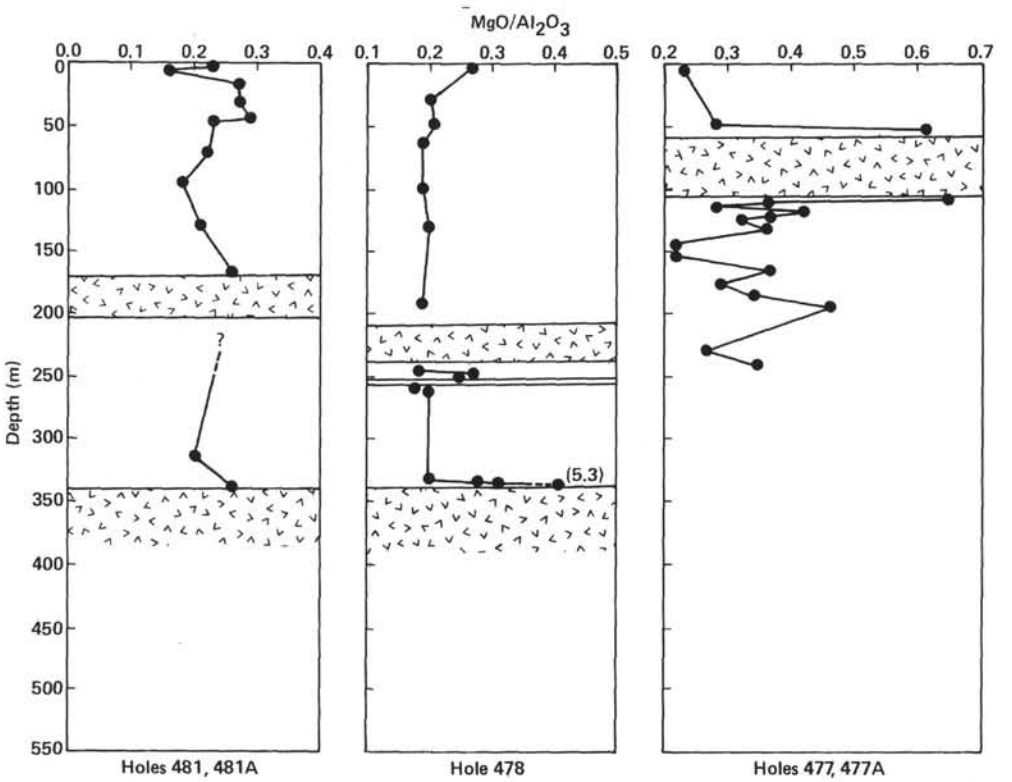

Figure 8. Geochemical trends for MgO at Sites 477, 478, and 481. Note the increase in MgO above and below sill in Holes 477, 477A.

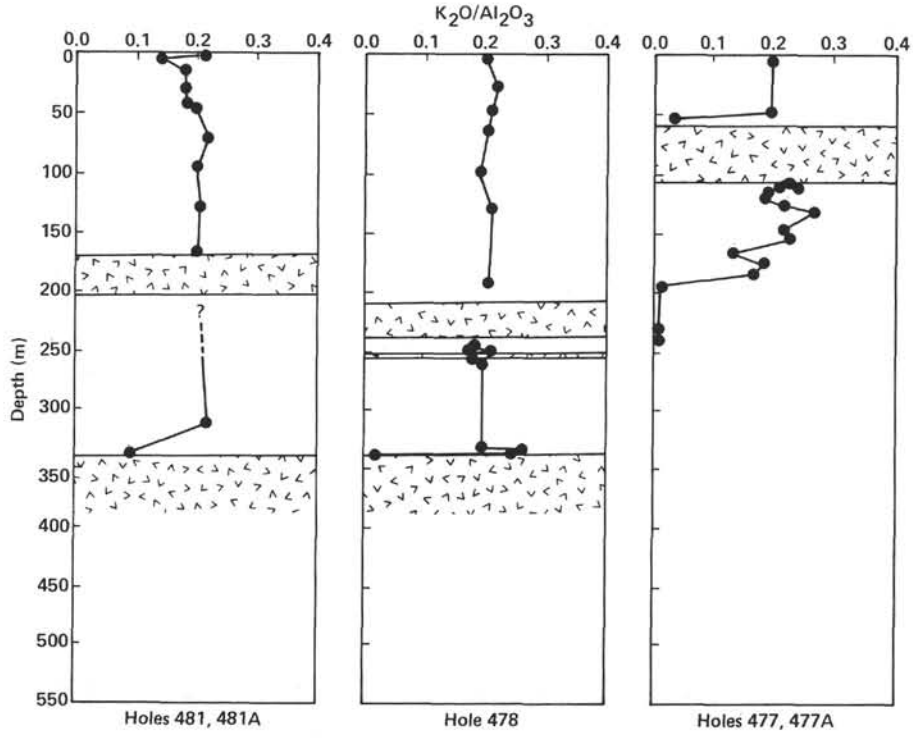

Figure 9. Geochemical trends for K_2O at Sites 477, 478, and 481. Note the near-quantitative removal of K_2O just above the sill and at bottom of hole at Site 477.

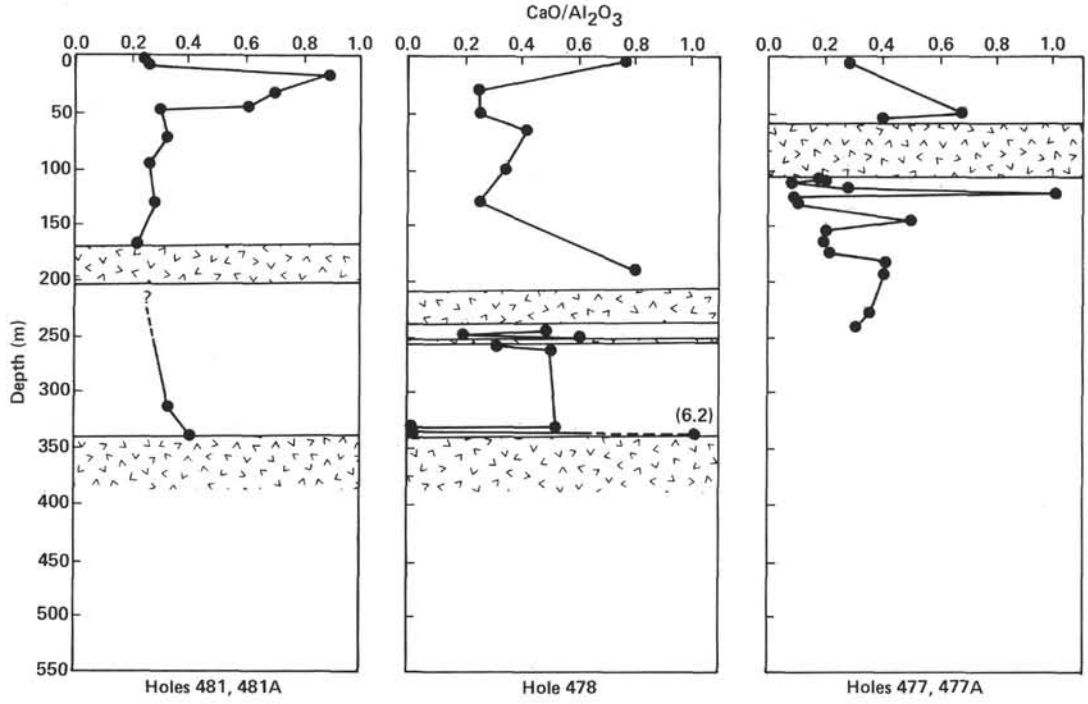

Figure 10. Geochemical trends for CaO at Sites 477, 478, and 481. Note sharp increase above upper sill and basement(?) at Site 478 because of the presence of dolomite and below sill at Site 477 because of anhydrite.

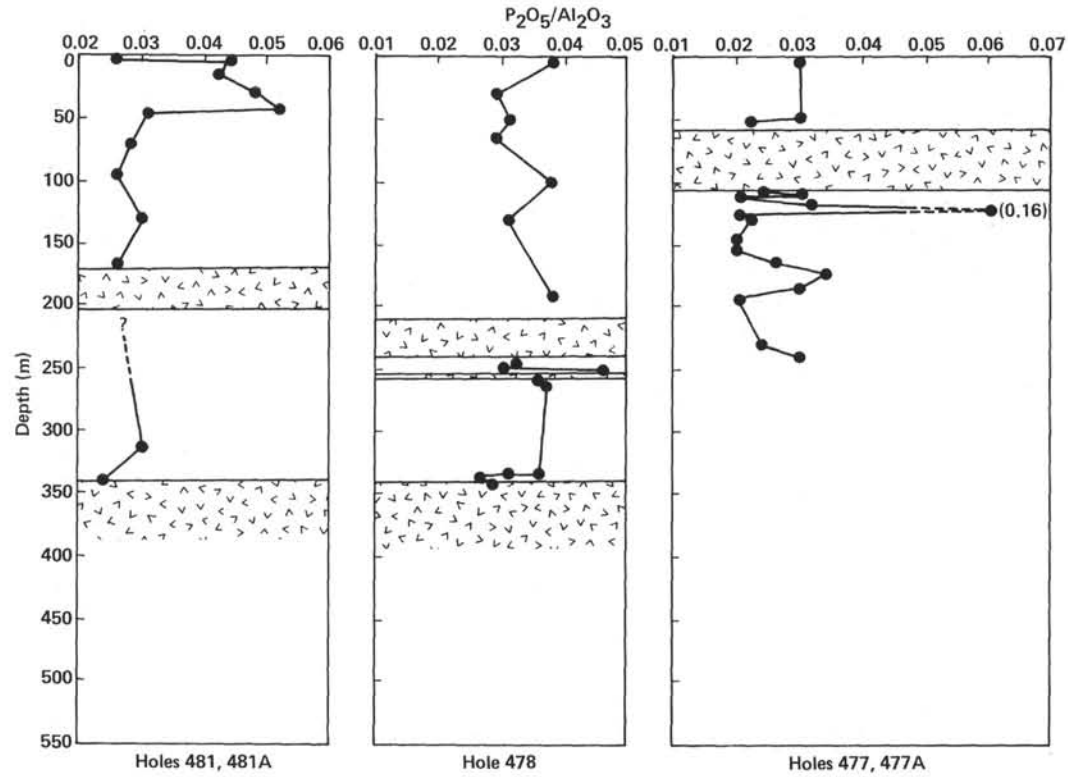

Figure 11. Geochemical trends for P_2O_5 at Sites 477, 478, and 481.

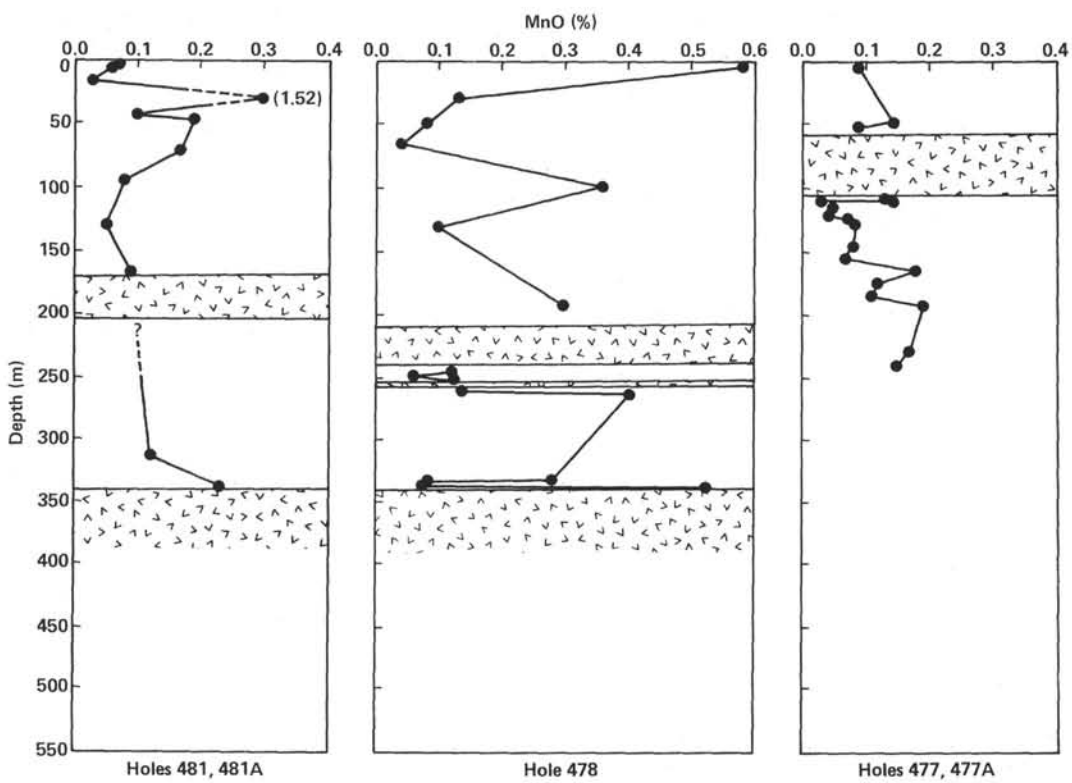

Figure 12. Geochemical trends for MnO at Sites 477, 478, and 481.

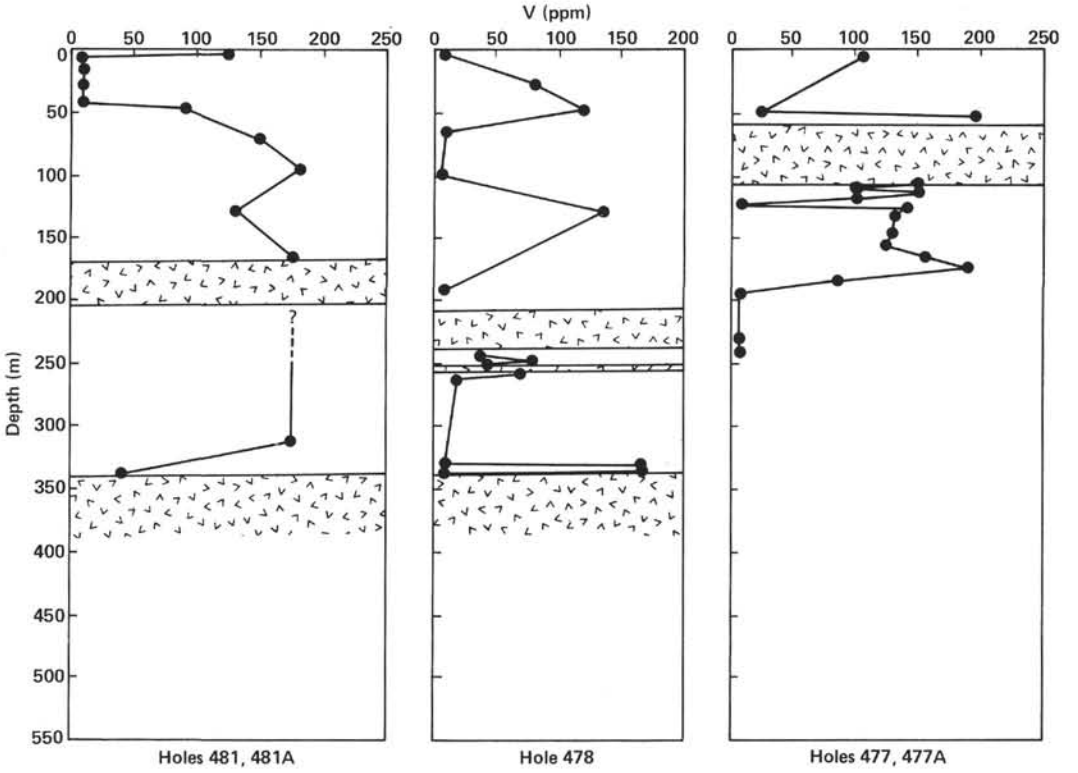

Figure 13. Geochemical trends for V at Sites 477, 478, and 481.

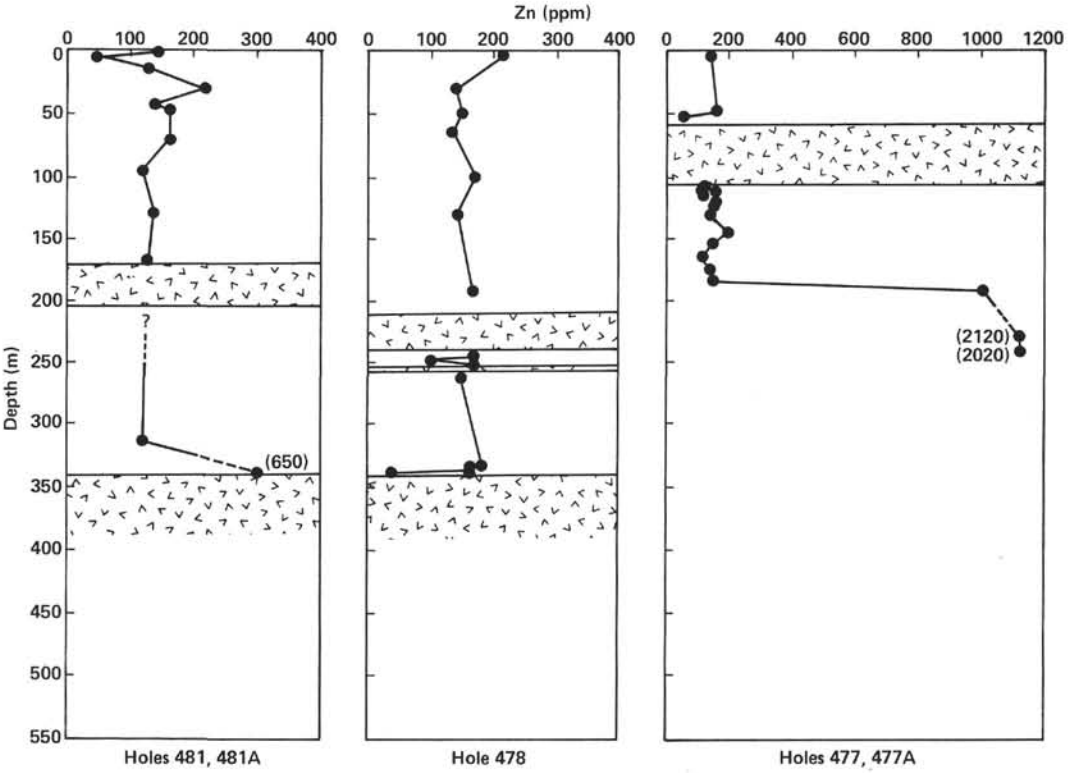

Figure 14. Geochemical trends for Zn at Sites 477, 478, and 481. Note sharp increase at bottom of hole at Site 477 and moderate increase at basement at Site 481.

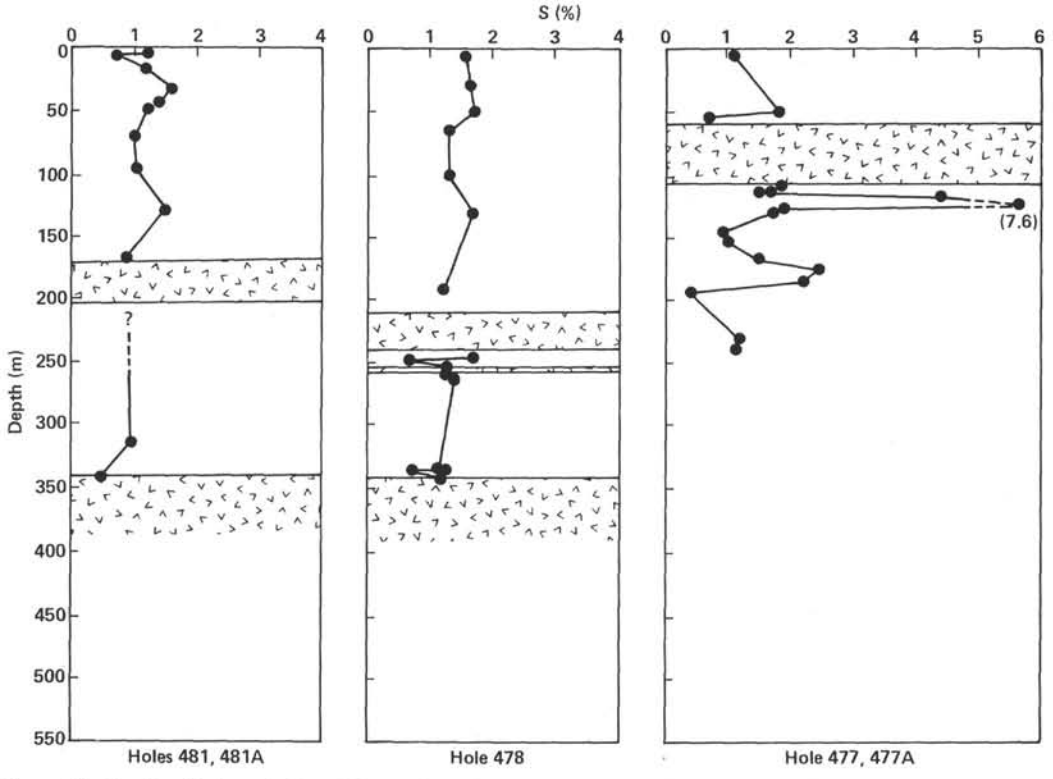

Figure 15. Geochemical trends for sulfur at Sites 477, 478, and 481. Note zone of high S just below sill at Site 477 because anhydrite is a dominant phase.

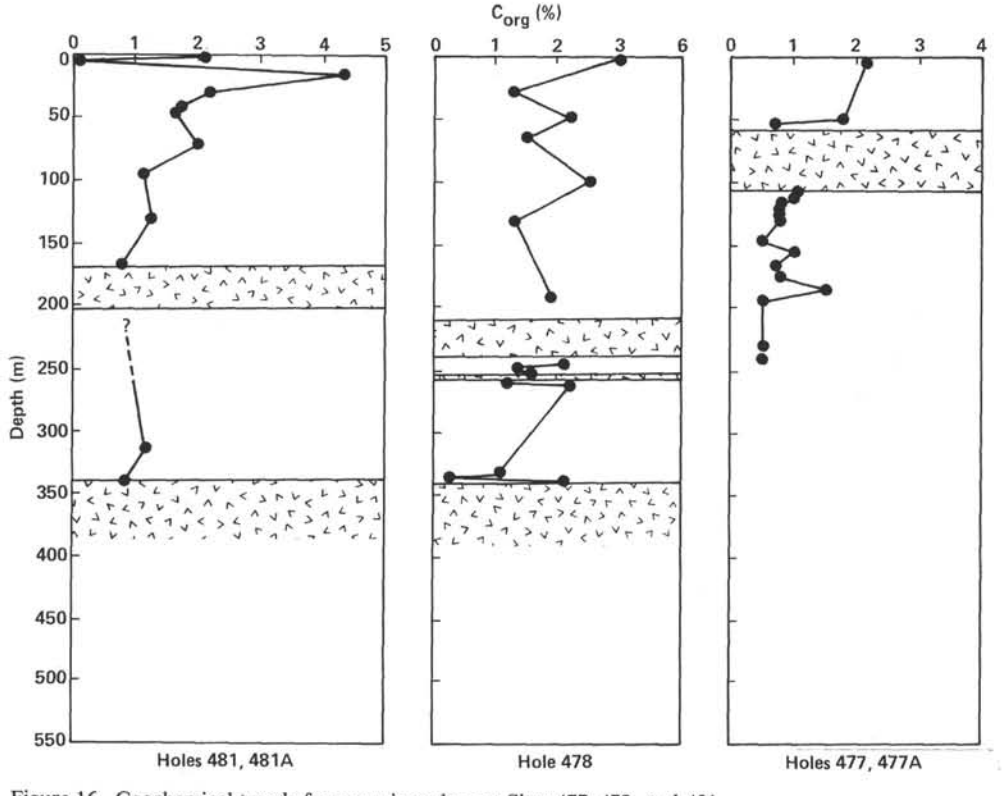

Figure 16. Geochemical trends for organic carbon at Sites 477, 478, and 481.

and S (Fig. 15) are exceptionally high. Fe_2O_3 and CaO are significantly above average and V is almost quantitatively removed. MgO, however, shows no deviation from average. The cause appears to encompass both a mineralogic and sedimentologic explanation. Mineralogically, anhydrite is a dominant phase, in some samples estimated at 70%; this explains the high CaO and S concentrations. The occurrence of pyrite as a secondary phase explains the increased Fe_2O_3 content. V appears to be deficient because of a dilution effect from the dominant anhydrite phase rather than because of hydrothermal removal (bottom of Hole 477). Elevated P_2O_5 in iron-rich sediments might imply an adsorption process of the kind suggested by Berner (1973). Alternatively, the high P_2O_5 content may be due to a concentration of fish debris, which was observed throughout the core. The latter seems a more convincing explanation given the nature of the departure from the average at the site and the lack of a parallel P_2O_5/Al_2O_3 trend with higher Fe_2O_3 at the base of the sediment column at Site 477.

Zinc (Fig. 14), Fe_2O_3, CaO, and MgO are the only elements or oxides showing significant increases with depth in the three Guaymas Basin sites. All indications suggest a hydrothermal origin for these trends. Hydrothermal dolomite explains the elevated MgO and CaO concentrations. The exact nature of the Fe and Zinc phases is, however, somewhat more vague. Possibilities include Fe-rich epidotes and Fe oxide cements. Pyrite, although present only in trace amounts, also contributes. The total Fe in the sediments appears to be derived from two sources: Fe adsorbed on terrigenous clays and Fe-bearing hydrothermal solutions. The geochemical trend at Site 477 suggests that the hydrothermal component increases proportionally with depth.

Zn concentrations in basal sediments are an order of magnitude higher at Site 477 and threefold higher than the average at Site 481. Though no Zn-bearing phases were detected with the pyrrhotite, the excess Zn may reside as a coprecipitate (ZnS). The major occurrence of sphalerite in the 21°N East Pacific Rise hydrothermal deposits to the south (Hekinian et al., 1980) lends credence to this possibility. Results from diabase–seawater interaction experiments (Seyfried and Bischoff, 1981) at 300°C and 500 bars with high water/rock ratios suggest a source for trace metals including Zn. High concentrations of Zn and other heavy metals were detected in the low-*p*H "sea-water" fluid soon after interaction began. Subsequently, the trace metal concentrations decrease as *p*H increases, producing final products such as Fe–Mn oxyhydroxides and Fe–Mg silicates similar to deposits of the Galapagos Mounds area. Sulfur is abundant, being derived from basaltic sources at depth (Site 477) as well as from biogenic matter (Shanks and Niemitz, this volume, Pt. 2). Fe–Mn oxyhydroxides and Fe–Mg silicates are not abundant in the altered sediments owing to the absence of suitable conditions for formation, the very great volume of sediment to be altered, and the highly diluted nature of the alteration products. In contrast, Mottl et al. (1979) suggest that sea water, when heated to >400°C, might transport heavy metals such as Zn in solution under conditions where water/rock ratios are lower. The characteristics of this system—temperature (T°), water/rock ratio, pressure (*P*), and sill implacement—are clearly transitory and hence difficult to deduce at present. This leads one to the conclusion that the inundation of new oceanic crust by anoxic, chemically reactive hemipelagic sediment plays a fundamental role in heavy metal transport and deposition.

At Site 477, MnO (Fig. 12) concentrations remain within a factor of two of the average for TM, showing no significant increase with depth or near the sill. Site 478 shows considerably more variation in concentration. Above the sills this variation can be attributed to oxidation-reduction conditions. Those sediments containing high MnO concentrations are associated with basal sands and silts of turbidites or bioturbated (relatively oxic) zones. Those with lower MnO values are associated with the clay-rich upper parts of turbidites, which tend to be reducing (H_2S odor, olive green color, faint laminae). In Sections 478-22-3 and 478-40-3, the trend of MnO seem to parallel that of MgO and CaO. Again dolomites were recovered from just above the upper sill, suggesting uptake of MnO, with MgO and CaO, from pore waters or the adsorption of Mn^{2+} on clay particles. An increase in MnO is not observed between the upper and lower sills, most likely because the Mn is largely located in interstitial water (Gieskes et al., this volume, Pt. 2). However, just below the lower sill in Section 478-30-2, there is another increase that is not associated with the altered sediments found in Section 478-30-1. MnO in Section 478-30-2 appears to be diagenetically enriched and unaffected by the intrusion of the small sill. The decrease in MnO in Sections 478-40-1 and 478-40-2 corresponds with the increase in indicators of reducing conditions.

Site 479 (Figs. 17–20)

Except for Samples 479-17-4, 59–61 cm and 479-39-2, 130–132 cm, little variation in sediment chemistry with depth is observed. The deviations from the average (Table 4) for one or both samples are common for all elements analyzed except V and CaO.

A departure from typical hemipelagic sediment components explains the chemical deviations in both samples. A rhyolitic ash layer found in Section 479-17-4 explains the above-average SiO_2 and K_2O concentrations; there are lesser increases in Fe_2O_3, MgO, Na_2O, MnO, and P_2O_5. The sediment sample from Section 479-39-2, also an ash deposit though of a somewhat altered basaltic variety, is more depleted in SiO_2, MgO, and Na_2O but quite enriched in Fe_2O_3, P_2O_5, and Ni. Under the microscope, this ash appears to be coated by what the chemical analysis suggests is an Fe oxide. The source of the Fe is most likely the surrounding sediments and interstitial fluids. Though the overall diagenetic environment is reducing, the low values of MnO and Fe_2O_3 imply that Fe in solution must be diffusing toward more porous and probably more oxic layers (note the low organic carbon content for this sample), where precipitation occurs as an oxide coating. Other elements, notably P_2O_5, Ni, and Co (not shown) appear to be scavenged from the interstitial waters during precipitation.

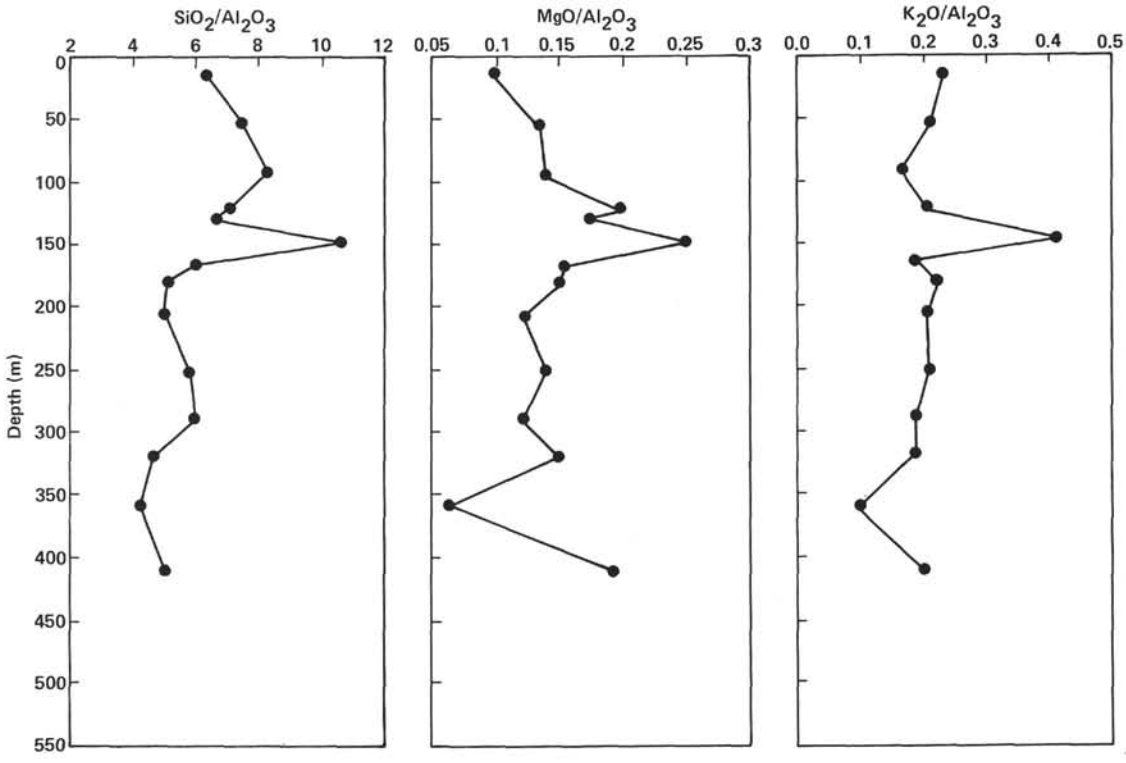

Figure 17. Geochemical trends for SiO_2, MgO, and K_2O at Site 479.

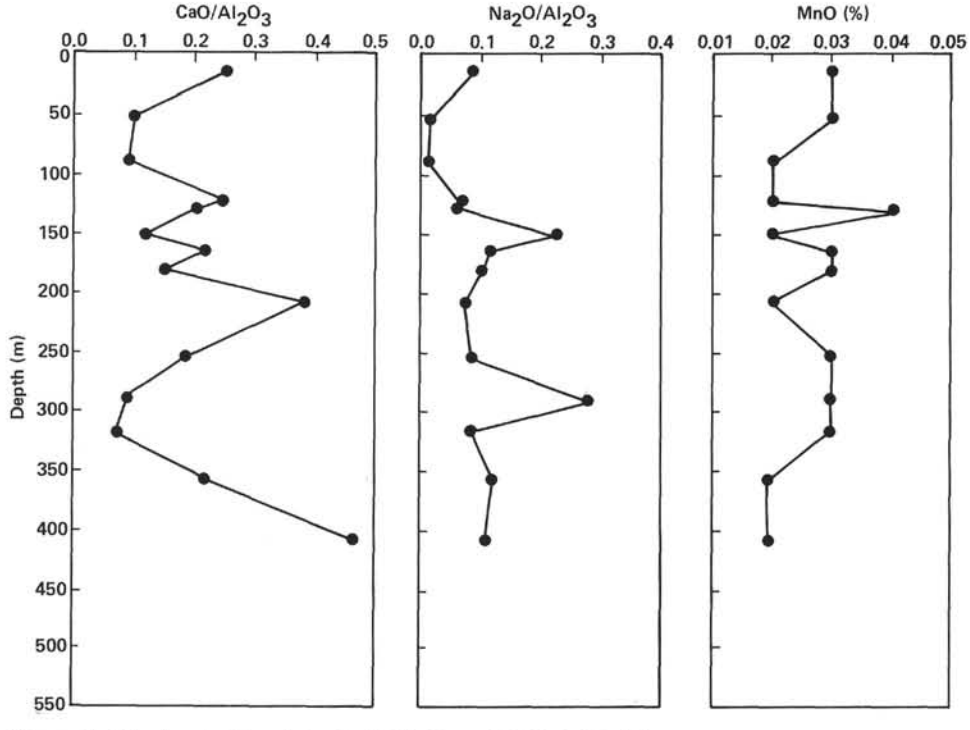

Figure 18. Geochemical trends for CaO, Na_2O, and MnO at Site 479.

Variations from the average CaO/Al_2O_3 ratios (Sections 479-23-6 and 479-44-4) are well correlated with high percentages of carbonate nannofossil ooze. The average Vanadium values are less than half the average of TM, probably because of dilution by V-deficient biogenous material.

DISCUSSION

Site 479 as Chemically "Average" Hemipelagic Sediment, Compared to Sites 477, 478, and 481

Located on the northeast slope of the Guaymas Basin, Site 479 lies within an oxygen-minimum zone (van

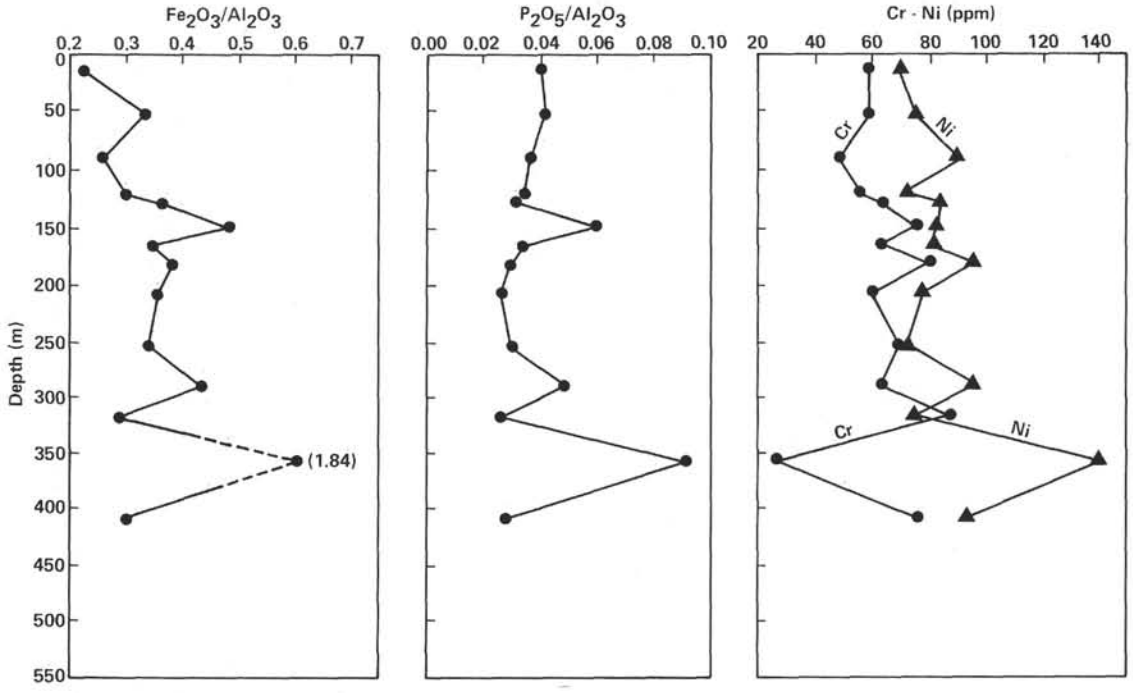

Figure 19. Geochemical trends for Fe_2O_3, P_2O_5, and Cr-Ni at Site 479.

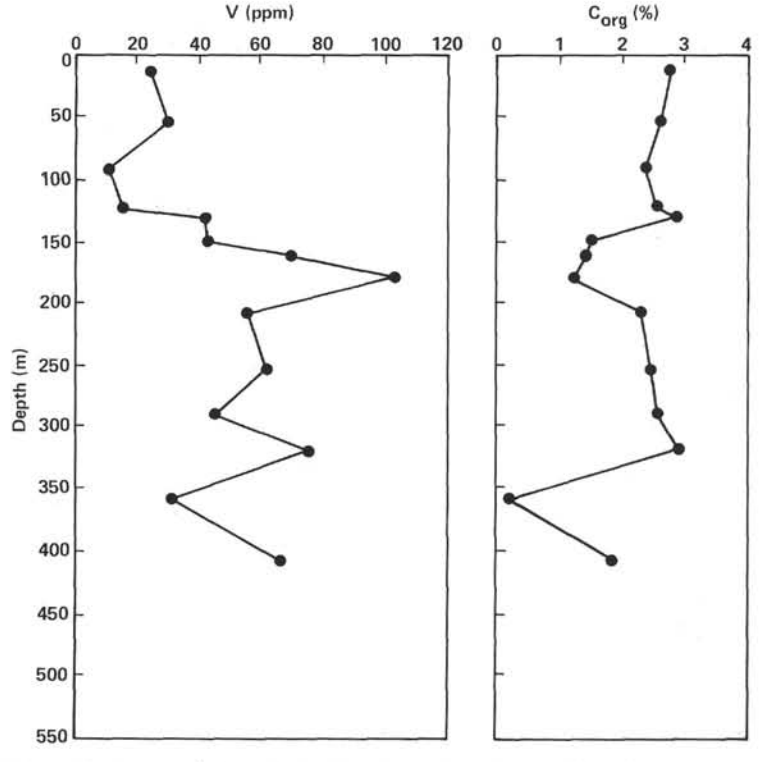

Figure 20. Geochemical trends for V and organic carbon at Site 479.

Andel and Shor, 1964) created by hydrographic and biologic processes. Stratigraphically, the site can be correlated with Site 480 using thin dolostone and ash layers at similar sub-bottom depths. Hole 479, although disturbed during the drilling process, contains sedimentary structures similar to Hole 480: rhythmically laminated diatom muds and diatomaceous oozes (mm-scale structures) alternating with thick (m-scale) homogeneous zones. Thus Holes 479 and 480 represent an undisturbed section of the continental slope environment which, it

is inferred, is a complete record of hemipelagic sedimentation over as much as 250,000 yr. (Crawford and Schrader, this volume, Pt. 2).

Are the geochemical trends for the major and minor elements in this complete sediment column representative of hemipelagic sediments? Is an average shale or empirically derived sediment (TM) more or less representative of the "average hemipelagic mud"?

Throughout this study, average shale and TM have been used as standards against which the geochemical trends of Leg 64 sites have been measured. Although a large percentage of hemipelagic sediment in any nearshore locality is derived from the weathering of continental rock (not necessarily of felsic composition), the use of so-called average shale or TM derived directly or through calculation from many rock analyses does not consider the biogenic component so important in Gulf of California sediments. This is clearly evident from a comparison of average shale and TM with the average SiO_2/Al_2O_3 values for all Leg 64 sites (Table 4). SiO_2/Al_2O_3 ratios for Sites 478–481 are approximately twice the average for shale and TM. Sites 474–476 and 477 exhibit lower SiO_2/Al_2O_3 because of (1) a lower percentage of siliceous fossils and (2) insufficient samples for statistically valid analyses. Furthermore, some of the SiO_2 depletion at Site 477 is due to hydrothermal processes. If this is so, then unaltered sediments above the sills at Sites 477, 478, and 481 should have average SiO_2/Al_2O_3 ratios closer to that for Site 479. With the exception of Site 477 (statistical bias), this is the case (Table 5). Similar averages for sediments above the sills in the "hydrothermal" sites have been calculated for all elements except Cl and S.

Among the major oxide ratios and MnO, greater similarities exist between Site 479 and Sites 477, 478, and 481 for SiO_2, K_2O and P_2O_5, whereas TM and the "hydrothermal" sites have similar averages for Fe_2O_3 and MnO. Na_2O and TiO_2 show little variation among all averages, whereas MgO and CaO averages for Sites 477, 478, and 481 differ from those of both TM and Site 479. Differences of the greatest magnitude occur among the minor elements, thus producing better general correlations among the DSDP sites than of any site with TM (Table 6).

The use of an "internal standard" such as Site 479 for defining the extent of hydrothermal activity in adjacent basinal sites is equivocal. Two major oxides ratios (SiO_2 and K_2O) that are considered to be diagnostic of hydrothermal processes are more like those at Site 479 than TM. MgO is the exception, being higher at the basinal sites than TM or at Site 479. An explanation for this excess probably involves the nature of sediment transport to the basin and the amount contributed from volcanic sources (Tortuga Island) and local basin flanks. Overall, the minor element averages show a better correlation with Site 479, particularly those that appear to be enriched or depleted because of hydrothermal processes (V and Zn).

Fe_2O_3 and MnO, useful as hydrothermal indicators, also show equivocal correlation with Site 479. MnO concentrations at Site 479 are an order of magnitude less than at the basinal sites because of the reducing conditions inherent in an oxygen-minimum zone. An alternative explanation is that the basinal sites are enriched in MnO relative to Site 479 because of hydrothermal processes. The geochemical trends for MnO above the sills in the basinal sites do not suggest such a universal enrichment, but rather the enrichments commonly seen in hemipelagic sediments with relatively oxygenated bottom waters (Li et al., 1969). Fe_2O_3 averages are not so significantly different as to be definitive.

The use of so-called "average" rocks and sediments for comparison with hemipelagic sediments appears valid only as a first approximation of the system. The concomitant use of an "internal" standard which more closely approximates the sediments under investigation (Aguayo, this volume, App. III) allows for even more viable comparisons. The proportions and sources of sediments at Site 479 are more closely matched with the hydrothermal sites than with TM or an average shale. Although some chemical ambiguities exist, the overall chemical character of sediments at Sites 477, 478, and 481 that are inferred to be unaltered is better correlated with Site 479 than with TM.

The Nature of the Guaymas Basin Hydrothermal System with Respect to Sedimentary Geochemistry

Hydrothermal talc–pyrrhotite–MnO_2 deposits occur along a fault scarp in the northern trough of the Guaymas Basin (Lonsdale, 1978). The discovery poses some questions about the nature of the "hydrothermal" system operating beneath a thin sediment cover. What is the source of the constituent elements which produce this deposit? What is the temporal and chemical influence of the sill injection process? What is the relationship between the sill injection and the larger magma source at depth with regard to alteration of sediments?

Table 5. Average major oxide ratios and elemental concentrations for unaltered sediments at Sites 477–481.

Sediment	SiO_2/Al_2O_3	Fe_2O_3/Al_2O_3	MgO/Al_2O_3	K_2O/Al_2O_3	CaO/Al_2O_3	Na_2O/Al_2O_3	TiO_2/Al_2O_3	P_2O_5/Al_2O_3	MnO (%)	Co (ppm)	Cr (ppm)	Cu (ppm)	Ni (ppm)	V (ppm)	Zn (ppm)
TM	3.81	0.42	0.16	0.17	0.24	0.11	0.046	0.012	0.115	22.5	100	50	79	125	85
Site 479 (N = 14)	6.26	0.45	0.15	0.21	0.20	0.10	0.047	0.040	0.026	10	63	46	66	48	141
Site 477 (N = 2)	4.39	0.38	0.26	0.20	0.45	0.12	0.051	0.031	0.115	10	54	42	55	66	151
Site 478 (N = 7)	6.08	0.39	0.27	0.21	0.43	0.10	0.049	0.034	0.21	8	47	47	44	55	159
Site 481 (N = 10)	6.12	0.37	0.23	0.19	0.41	0.09	0.047	0.036	0.24	8	44	43	45	89	141

Note: Terrigenous matter (TM) included for comparison.

Table 6. Correlation coefficients of Table 5 chemical data for Sites 477–481 and TM.

	TM	Site 479	Site 477	Site 478	Site 481
TM	1.000				
Site 479	0.800	1.000			
Site 477	0.806	0.988	1.000		
Site 478	0.738	0.979	0.993	1.000	
Site 481	0.838	0.947	0.983	0.953	1.000

The evidence for hydrothermal activity in the Guaymas Basin consists of the following:

1) Geochemical trends (as well as physical properties, color, etc.) below sills, particularly at Site 477, differ significantly from trends above the sills. All sediments may have initially been hemipelagic debris consisting of diatomaceous mud and mud turbidites.

2) Sediments immediately above and below sills exhibit large deviations from the average, suggesting that intrusions cause considerable geochemical change. This is not true for all elements or all sills sampled. Furthermore, the chemical data (Saunders and Fornari, this volume, Pt. 2) suggest only modest sill alteration.

3) The mineralogy noted below the sill at Site 477 is quite different from that seen in any "normal" hemipelagic sediment and includes anhydrite, calcite, dolomite, crystalline pyrite or pyrrhotite, epidote, authigenic quartz and albite, and newly formed chlorite (Kelts, this volume, Pt. 2).

4) Some sediments near sills have heavy metal concentrations, elevated as much as an order of magnitude above average shale.

5) Sulfur isotope values on mineral phases of pyrite, pyrrhotite, and anhydrite at Site 477 (Shanks and Niemitz, this volume, Pt. 2) indicate that hydrothermal processes are occurring at depth. Diagenetic/biogenous processes decrease in importance with depth below the sill.

6) Measured and extrapolated temperatures below the sill at Site 477 are consistent with changes in mineralogy and heat flow distribution determined from surface probes (Williams et al., 1979; Becker, 1981).

In contrast is the following evidence:

1) In general, the sediments cored at other basinal sites do not show geochemical trends similar to Site 477.

2) Measured heat flow at Sites 478 and 481 is high relative to average oceanic crust but very low compared to Site 477.

3) Site 481 is approximately 3 km southeast of the recently discovered "hydrothermal" deposit (Lonsdale et al., 1980) yet shows little hydrothermal alteration of the type exhibited at Site 477.

4) The geochemical character of MnO above sills at all basinal sites appears to be diagenetic, with enrichment in zones inferred to be relatively oxic and depletion in anoxic zones. Large increases in MnO do not occur as sills or basement are approached.

These observations suggest a complex hydrothermal system consisting of two interrelated parts. Each part produces characteristic geochemical signatures yet the system as a whole is ultimately caused by the same phenomenon, the divergence of a young and transient plate boundary. The overall driving mechanism for the system is the magma (source of heat and sill material) at depth. The existence of sills in all holes and the high heat flow distribution confirm this fact. Site 477 observations further corroborate heat flow models (Williams et al., 1979) suggesting a magma source close to the sea floor, which is in turn deluged and insulated by rapidly accumulating hemipelagic sediments. However, this heat source is not present at Sites 478 and 481, either because heating has ceased at these localities or because drilling was terminated in a thick sill rather than in basement, and more sediment (altered?) exists below this depth. The first alternative appears more likely, considering heat flow distributions in the basin. A reasonable analogy to active and inactive vents and chimneys in the Galapagos Mounds area can be envisioned. That the heat source appears ephemeral may explain the relative paucity of metalliferous deposits, discovered only by submersible exploration. Furthermore, transient heat sources seem consistent with the mechanisms of formation of an immature plate boundary (Niemitz and Bischoff, 1981; Bischoff and Henyey, 1974).

The role of the sills in the hydrothermal system appears to be twofold. The geochemical contrast between sediments above and below the sills, especially at Site 477, implies that sills act as lids on the convection of heat from below and so may intensify the hydrothermal processes, causing relatively high grades of metamorphism at relatively shallow depths. If we conceive that the sills are interfingered within the boundaries of the basin troughs and are of limited area, it is likely that there are localities where altered sediments may be found quite close to the sea floor because of gaps in the sill cover. In fact, such a locality has been probed near Site 477 (Stout, 1981). On the other hand, the sills injected into high-water-content sediments at shallow depths act as a short-term heat source (tens of years?) for a secondary hydrothermal system, causing at least two phenomena: (1) The injection itself causes rapid dewatering of surrounding sediments and decreased porosity (site chapters, physical properties, this volume, Pt. 1; Einsele, this volume, Pt. 2; Einsele et al., 1980). (2) These now hot interstitial waters, enriched in Mg, Mn, Fe, and S, escape up fault scarps to be precipitated as talc–pyrrhotite–MnO_2 deposits on the sea floor (Einsele et al., 1980; Lonsdale et al., 1980). The sedimentary geochemical trends and sill chemistry imply that the source of the constituents in the talc deposits is predominantly the sediment and interstitial waters within. Two lines of evidence support this assertion. The sills are only moderately altered, with minor vein alteration; they therefore appear not to be so leached of elements as has been observed in sea-water–basalt interaction experiments (Seyfried and Bischoff, 1981) or in oceanic tholeiitic basalt geochemistry (Humphris and Thompson, 1978a,b). Moreover, the sulfur isotope value reported for the metalliferous sea-floor deposit (−3.94‰ [CDT]; Lonsdale et al., 1980), when compared to values at Site 477 (Shanks and Niemitz, this volume, Pt. 2), suggests a mixture of basaltic and biogenic sulfur. The metallifer-

ous talc deposits, therefore, appear to result from interstitial waters, enriched in elements common to hemipelagic sediments, and driven to the surface along fault traces by the intrusion of sills at shallow depths.

CONCLUSIONS

1. The sedimentary geochemical results from Leg 64 may be grouped into those derived from characteristic hemipelagic diatom muds and mud turbidites and those which show effects of hydrothermal (or contact-zone) alteration of these sediments and associated sills.

2. The sedimentary geochemistry of Sites 474–476 is similar and clearly reflects changes in abundance of sedimentary components (biogenous versus terrigenous) and mineralogy.

3. The mineralogy and corresponding chemistry below the sills in Holes 477 and 477A suggest an active hydrothermal system operating in close proximity to the sea floor, not in contact with sea water but within a thin covering of rapidly accumulating sediments.

4. The lack of similar mineralogy below sills at Sites 478 and 481 suggests little hydrothermal activity. Alternatively, the system may reside below sills not drilled.

5. Evidence for a heat source at depth at Site 477, the presence of cold, dolerite sills in the sediment column, and the occurrence of hydrothermal deposits on the sea floor suggest a complex hydrothermal system. The deep heat source drives the crustal plates apart yet appears to be as transient as the young and constantly readjusting plate boundary. The sills act as a secondary and short-term source of heat, causing dewatering of the sediments and probably formation of small, localized hydrothermal deposits on the sea floor. The source for the components in these deposits appears largely to be the sediments and interstitial water. The primary role of the sills is to effectively confine the heat and circulating fluids, causing significant alteration of hemipelagic sediments at shallow depths.

6. Geochemical trends at Sites 479 and 480 remain essentially uniform with depth, suggesting that Site 479 can be regarded as an "internal" standard against which the degree of hydrothermal alteration in adjacent basinal sites can be measured.

ACKNOWLEDGMENTS

I wish to thank the scientific staff and technicians aboard *Glomar Challenger* for their help with sampling and their stimulating discussion regarding this study. Assistance and use of equipment for performing the chemical analyses on the sediments were provided by the USGS Analytical Branch in Menlo Park, California; for this help I am most grateful. Finally, I am grateful to Dr. James Bischoff of the USGS Marine Geology Branch for moral and financial support while performing the analyses. This research was supported in part by the Dickinson College Research and Development Fund; a Research Corp., Cottrell College grant; and the USGS. David Kadter, Jim Bischoff, Joris Gieskes, and Kerry Kelts reviewed the manuscript and provided many helpful suggestions for improvement.

REFERENCES

Becker, K., 1981. Heat transfer at spreading centers of the Guaymas Basin, Gulf of California. *Geol. Soc. Am. Abstr. Prog.*, 13 (no. 2):44.

Berner, R. A., 1973. Phosphate removal from seawater by adsorption on volcanogenic ferric oxides. *Earth Planet. Sci. Lett.*, 18:77–86.

Bischoff, J. L., and Henyey, T. L., 1974. Tectonic elements of the central part of the Gulf of California. *Geol. Soc. Am. Bull.*, 85: 1893–1904.

Boström, K., Joensuu, O., and Brohm, I., 1974. Plankton—its chemical composition and its significance as a source of pelagic sediment. *Chem. Geol.*, 14:255–271.

Boström, K., Joensuu, O., Valdes, S., Charm, W., and Glaccum, R., 1976. Geochemistry and origin of East Pacific sediments sampled during Leg 34. *In* Yeats, R. S., Hart, S. R., et al., *Init. Repts. DSDP*, 34: Washington (U.S. Govt. Printing Office), 559–574.

Calvert, S. E., and Price, N. B., 1970. Minor metal content of recent organic rich sediment of Southwest Africa. *Nature*, 227:593–595.

Einsele, G., Gieskes, J. M., Curray, J., Moore, D., Aguayo, E., Aubry, M.-P., Fornari, D., Guerrero, J., Kastner, M., Kelts, K., Lyle, M., Matoba, Y., Molina-Cruz, A., Niemitz, J., Rueda, J., Saunders, A., Schrader, H., Simoneit, P., and Vacquier, V., 1980. Intrusion of basaltic sills into highly porous sediment and resulting hydrothermal activity. *Nature*, 283:441–445.

Flanagan, F. J., 1972. 1972 values of international geochemical reference samples. *Geochim. Cosmochim. Acta*, 37:1189–1200.

_____, 1976. *Descriptions and Analyses of Eight New USGS Rock Standards.* U.S. Geol. Surv. Prof. Paper 840: Washington (U.S. Govt. Printing Office).

Hekinian, R., Fevrier, M., Bischoff, J. L., Picot, P., and Shanks, W. C., 1980. Sulfide deposits from the EPR near 21°N. *Science*, 207: 1433–1444.

Hoagland, J R., and Elders, W. A., 1978. Hydrothermal mineralogy and isotope geochemistry in the Cerro Prieto Geothermal Field, Mexico. I. Hydrothermal mineral zonation. *Trans. Geotherm. Resourc. Counc.*, 2:283–286.

Humphris, S. E., and Thompson, G., 1978a. Hydrothermal alteration of oceanic basalts by seawater. *Geochim. Cosmochim. Acta*, 42: 107–127.

_____, 1978b. Trace element mobility during hydrothermal alteration of oceanic basalts. *Geochim. Cosmochim. Acta*, 42:127–137.

Krauskopf, K. B., 1979. *Introduction to Geochemistry* (2nd ed.): New York (McGraw-Hill).

Lawver, L. A., Williams, D. L., and Von Herzen, R. P., 1975. A major geothermal anomaly in the Gulf of California. *Nature*, 257: 23–28.

Li, Y. H., Bischoff, J. L., and Mathieu, G. G., 1969. The migration of Mn in Arctic Basin sediments. *Earth Planet. Sci. Lett.*, 7: 265–270.

Lonsdale, P., 1978. Submersible exploration of Guaymas Basin: A preliminary report of the Gulf of California 1977 operations of DSV-4 *SeaCliff*. Scripps Inst. Oceanog. Ref. 78–1.

Lonsdale, P., Bischoff, J. L., Burns, V. E., Kastner, M., and Sweeney, R. E., 1980. A high temperature hydrothermal deposit on the seabed at a Gulf of California spreading center. *Earth Planet. Sci. Lett.*, 49:8–20.

Mottl, M. J., Holland, H. D., and Corr, R. F., 1979. Chemical exchange during hydrothermal alteration of basalt by seawater—II. Experimental results for Fe, Mn, and sulfur species. *Geochim. Cosmochim. Acta*, 43:869–884.

Niemitz, J. W., and Bischoff, J. L., 1981. Tectonic elements of the southern part of the Gulf of California. *Geol. Soc. Am. Bull.*, Pt. 2, 92:360–407.

Seyfried, W. E., Jr., and Bischoff, J. L., 1981. Experimental seawater-basalt interaction at 300°C, 500 bars, chemical exchange, secondary mineral formation and implications for the transport of heavy metals. *Geochim. Cosmochim. Acta*, 45:135–148.

Stout, P., 1981. Near surface sediments affected by high heat flow in the Guaymas Basin, Gulf of California. *Geol. Soc. Am. Abstr. Prog.*, 13(no. 2):108.

van Andel, Tj. H., and Shor, G. G., 1964. *Marine Geology of the Gulf of California:* Am. Assoc. Pet. Geol. Mem. 3: Tulsa (AAPG).

Williams, D. L., Becker, K., Lawver, L. A., and Von Herzen, R. P., 1979. Heat flow at the spreading centers of the Guaymas Basin, Gulf of California. *J. Geophys. Res.*, 84:6757–6769.